ORIGINAL ARTICLE

METROECONOMICA
INTERNATIONAL REVIEW OF ECONOMICS

WILEY

Segregation with social linkages: Evaluating Schelling's model with networked individuals

Roy Cerqueti[1,2] | Luca De Benedictis[3,4,5] |
Valerio Leone Sciabolazza[6]

[1]Department of Social and Economic Sciences, University of La Sapienza, Rome, Italy

[2]School of Business, London South Bank University, London, UK

[3]Department of Economics and Law, University of Macerata, Macerata, Italy

[4]Rossi-Doria Center, University Roma Tre, Roma, Italy

[5]Department of Business and Management, Luiss, Rome, Italy

[6]Department of Economics and Business and Research, University of Naples Parthenope, Napoli, Italy

Correspondence
Valerio Leone Sciabolazza, Department of Economics and Business and Research, University of Naples Parthenope, Naples 80132, Italy.
Email: valerio.leonesciabolazza@uniparthenope.it

Abstract

This paper generalizes the original Schelling model of racial and residential segregation to a context of variable externalities due to social linkages. In a setting in which individuals' utility function is a convex combination of a heuristic function *à la* Schelling, of the distance to friends, and of the cost of moving, the prediction of the original model gets attenuated: the segregation equilibria are not the unique solutions. While the cost of distance has a monotonic pro-status-quo effect, equivalent to that of models of migration and gravity models, if *friends* and *neighbors* are formed following independent processes, the location of friends in space generates an externality that reinforces the initial configuration if the distance to friends is minimal, and if the number of friends is high. The effect on segregation equilibria crucially depends on the role played by network externalities.

KEYWORDS
Schelling's Segregation Model, Networks, Network externality

JEL CLASSIFICATION
B55; D62; D85; D90

1 | INTRODUCTION

A basic organizing principle of social relations is the tendency of people to associate with others who are similar to themselves. This observed propensity towards homophily leads to different forms of segregation, which have been long studied both from the economic literature (Jackson, 2007) and the sociological literature (McPherson et al., 2001).

A prominent contribution to the understanding of the dynamics of segregation is that by Schelling (1969, 1971a, 1971b). The logic of Schelling's argument offers a simple and subtle intuition to racial residential segregation: homophily, in spite of individual preferences being characterized by the desire for integration, generates a completely unexpected social equilibrium where individuals tend to live within racially homogenous communities. The model devised by Schelling thus leads to the conclusion that radical racial segregation is a robust and stable equilibrium even if individuals prefer moderate racial integration.

Building on this framework, large research has been conducted to document and understand the determinants of racial and residential segregation across several European countries (Baerveldt et al., 2004; van Ham et al., 2016; Vermeij et al., 2009), in the United States (Batty, 2013; Clark, 1991; Henderson, 2014; Möbius & Rosenblat, 2001), and Israel (Hatna & Benenson, 2012). However, empirical findings rarely proved Schelling's prediction of extreme racial spatial separation and ghettos to be correct (Easterly, 2009; Ong, 2017). Also in the United States, which ultimately inspired Schelling's work[1] and most of the research in this field, despite ethnic segregation remains still prevalent in many cities (Logan & Stults, 2011), it has significantly decreased over the last 40 years (Glaeser & Vigdor, 2012), and the conformation of cities and urban areas is becoming as various as it possibly could be. US census data strongly confirms this pattern, as it is shown in Figure 1. The figure reports a standard measure of urban segregation, the dissimilarity index of the black and white communities in the US metropolitan regions for each census year from 1940 to 2010. This metric has a support that goes from 0 (perfect integration) to 100 (perfect segregation). Specifically, the value reported in the figure is a weighted average of the dissimilarity index for all metropolitan regions in a census year, with weights given by the total population in the regions (additional details are provided in the caption of the figure). The trend in the value of this metric clearly shows that segregation has remarkably weakened since the 1970s.

This evidence for a general pattern of mitigated segregation, still unexplained by Schelling's work and its extensions, cast doubts on the ineluctability of what the model posits, and calls for additional research. Complementing Schelling's rational, this paper proposes to contribute to fill this gap in the literature by proposing a framework to unravel what forces might contrast dramatic population moves and produce the emergence of limited segregation equilibria.

To this purpose, Schelling's heuristic is put in interplay with a positive cost of moving and, more importantly, the presence of social linkages. This minimal departure from Schelling's model provides the conditions under which multiple equilibria (i.e., mixed segregation) arise. The reason is that social connections affect how decisions are distributed within the society (Calvo-Armengol & Jackson, 2004, 2007), and introduce a form of heterogeneity across agents which can change the pattern of equilibria dictated by Schelling's model (Jackson, 2007). In fact, provided that agents are sensitive to being located close to their social connections, and not all of them might be formed within one's group, different types of group compositions may be observed in a neighborhood. However, if moving costs constrain relocation choices, and not all neighborhoods are equally accessible to agents, we will observe the rise of zone

---

[1]Quoting Schelling: "My ultimate concern of course is segregation by color in the United States" Schelling (1969, p. 488).
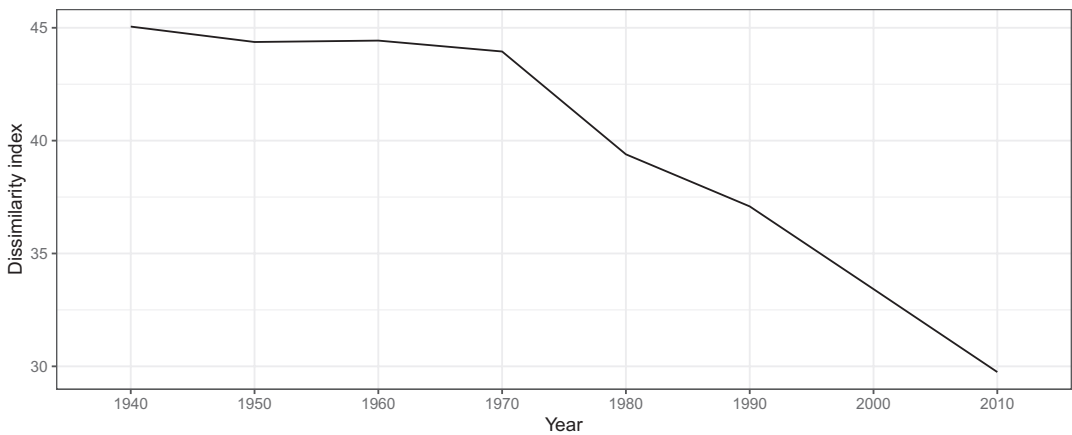
FIGURE 1 Ethnic segregation in the metropolitan regions of the United States. For each census year (*x*-axis), we report the value of the dissimilarity index for the Black and White communities residing in the United States (*y*-axis). The index is obtained with the formula $0.5 * \sum_i |\frac{b_i}{B} - \frac{w_i}{W}|$, where b_i and w_i indicate, respectively, the Black and White population in census tract i, while B and W registers, respectively, the Black and White population in the metropolitan region to which i belongs. The value reported in the figure is the weighted average of the dissimilarity index for all metropolitan regions in a census year, with weights given by the total population in the regions. *Source*: The authors' elaboration from US census data

of competition and contestation, making the outcome of Schelling's model uncertain (Silver et al., 2021), and dependent on the location of agents and their sensitivity to others' relocation decisions.

Therefore, while Schelling considers the case when people identify only with one of their characteristics (e.g., ethnicity), we allow for the possibility that the force of attraction determined by homophily is affected by different identities (e.g., ethnicity and social connections) and mitigated by the cost of moving. In what follows, we will show how this generalization provides a valuable insight on the formation of racially mixed neighborhoods as they result from both local inertia, generated by the incidence of moving costs, and network externalities, arising from the desire to live close to friends. In our setup, the interplay between moving costs and social linkages generates a network externality that has an effect on the segregation patterns. When the agent is able to move and simultaneously reduce the average distance from her friends, incentives to relocate to a segregated area will decrease for everyone. After the move, incentives to modify their location will decrease for friends close to the agent, and will increase for all the others. Consequently, the market equilibrium in residential location and the subsequent level of social segregation will depend on economic factors (the cost of moving), identity (groups and the importance of homophily), and social linkages (friends, their choices and the willingness to minimize the spatial distance between individual residence and the residence of friends).

The remainder of the paper is organized as follows. In Section 2, we discuss the literature related to our work. In Section 3, we show how Schelling's model can be expanded so to include the effects played by network externalities and moving costs. The components of this model are further explicated in Section 4, where we detail how they can be used to investigate segregation equilibria in a simulated setting. Section 5 presents the results of such simulations. Finally, Section 6 concludes.

2 | LITERATURE REVIEW

Outlined in a series of papers (Schelling, 1969, 1971a, 1971b) and further elaborated in Schelling (2006), Schelling's theory provided the foundation for large research in economics (Benito-Ostolaza et al., 2015; Lee, 2004; Rosser, 2011; Sethi & Somanathan, 2004), sociology (Benard & Willer, 2007; Benenson et al., 2009; Fossett, 2011; Zhang, 2004), and social network analysis (de Marti & Zenou, 2017; Henry et al., 2011; Stadtfeld & Vörös, 2020).

Schelling's simple mechanism was originally framed as a heuristic process of strategic reasoning, in which people leave their residence whenever they are a too small minority in their neighborhood.[2] Both versions of the Schelling model, the "chequerboard model"—in which a fixed number of agents belonging to two different groups (the "reds" and the "blue" ones) choose where to locate on a grid (or on a line, if the chequerboard space is reduced to a single row) as a consequence of their heuristic—and the "neighborhood tipping model"—in which a small change in group composition of a neighborhood can put the heuristic in motion, and leads to an accelerating and irreversible dynamic process bringing to racial segregation—are based on the same stringent logic in which observed *macrobehavior* clashes with *micromotives*. We briefly recall Schelling's reasoning through an illustrative example for the reader's convenience, and discuss the rational underlying it.

2.1 | An example: Schelling "chequerboard model" without social linkages

Consider Figure 2, in which 74 individuals are located on a 10×10 grid. 37 of them are "reds," and 37 are "blues."

The 26 spots, that are not occupied neither by reds nor by blues, remain empty, and can be occupied in a subsequent round of play. Finally, the initial position of each individual is random.

Each individual has up to eight adjacent neighbors and has a preference over homophily. Following a heuristic process, the generic individual remains in her location as long as at least a share x of her neighbors are of the same type as she is. In this example, we set $x = 1/3$. Let us now consider individual 23 in Figure 2.[3] Individual 23 is red and is surrounded by six reds and two empty spots. Since empty cells are excluded from the heuristic accounting, individual 23 compares $6/6 > 1/3$ and she decides not to move from her position on the grid. Individual 45, instead, is red as well but is surrounded by four blues, one red, and three empty spots. Since $1/5 < 1/3$ she will move from her position on the grid. Similarly, all unhappy individuals will move to an empty spot that satisfies the "at least one-third" heuristic. Segregation will rapidly emerge.[4]

---

[2]The same reasoning has been proposed using different setups and the main findings of the model were found consistent regardless of the definition of the neighborhood and its topography (Taylor, 1984).

[3]In Schelling's original settings all agents unsatisfied of their location simultaneously put their name on a list, and then they move according to an empty space following some arbitrary order. Successively, a new list is drawn and the process repeats until no agents have further incentive to move. Here, this process is simplified to avoid unnecessary complexities, and we select one agent randomly.

[4]All possible multiple-equilibria are stable and segregation can be reduced only introducing a distaste for uniformity, corresponding to a heuristic > 1/3 and < 7/8, as an example. The formulation is analogous to Atkinson (1970) inequality aversion.
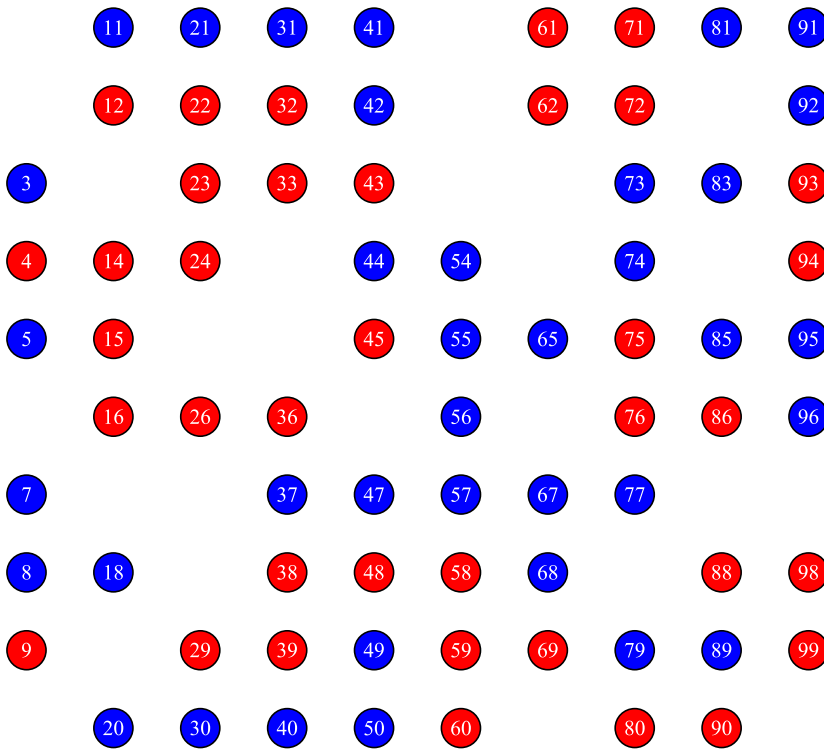
FIGURE 2   The Schelling "chequerboard" model [Colour figure can be viewed at wileyonlinelibrary.com]

2.2 | Related literature

Schelling's model has been also decontextualized, put in close analogy to concepts originated in other disciplines (Vinković & Kirman, 2006), and extended so that its heuristic and other choice variables (Hensher et al., 2005) could be included in a compact multivariate utility function. Among the many, Sethi and Somanathan (2004) defines a framework in which agents care about both the racial composition and the affluence of neighborhoods, showing that, in a context of multiple equilibria, a reduction in inequality can be observed both with a *rise* in segregation or a *fall* in the level of affluence, depending on the speed of income convergence. Zhang (2004) instead, considers the existence of a housing market and agents chose to move according their heuristic and the price of an empty spot.[5]

As in Pancs and Vriend (2007), we build our contribution around the original Schelling "chequerboard model," in which the number of individuals and their characteristics are well defined and the number of neighborhoods is higher than one. Indeed, even if the two Schelling's formalizations—the "neighborhood tipping model" and the "chequerboard model"—can be combined into one single theoretical framework (see, e.g., Young, 2001; Zhang, 2011 and the excellent textbook treatment of the models by Ioannides, 2013 and Easley & Kleinberg, 2010), this approach would add unnecessary complexities to our work. By contrast, we aim at keeping the details of this work as simple as possible.

---

[5]Our model can naturally encompass extensions that expand the choice set of individuals, such as those of the above contributions.
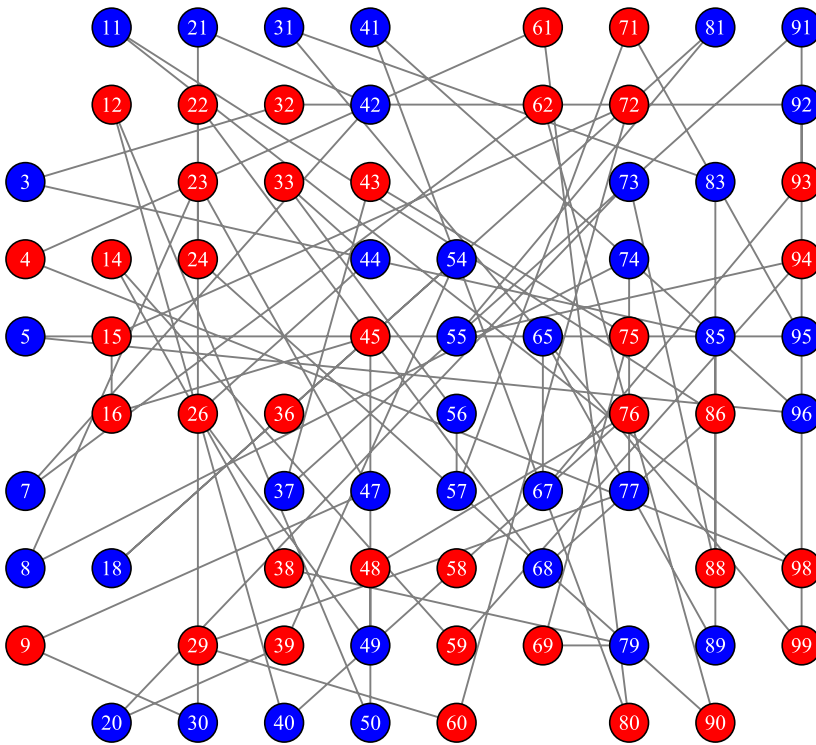
FIGURE 3 The Schelling "chequerboard" model with networked individuals. The setup is similar to the one in Schelling (1969, 2006) [Colour figure can be viewed at wileyonlinelibrary.com]

Albeit analytically different, this line of research has strong connections with the literature originated by the seminal contribution of George Akerlof and Rachel Kranton on the Economics of Identity (Akerlof & Kranton, 2000) and summarized and popularized in Akerlof and Kranton (2012). In their framework, agents make their choice according to the standard utility maximization apparatus—market prices, individual income, and preferences—*and* an identity variable, depending on individual characteristics (e.g., being female, being White, being homosexual) and self-image, on the social context and on the behavior of others. Choices depend therefore on economic incentives and identity issues.

3 | SCHELLING MODEL WITH NETWORKED INDIVIDUALS

In our model, we consider a situation similar to that described in Figure 2. Agents are located at random in space, and they are also similarly split in two different groups, the "reds" and the "blues," but, with respect to Schelling's original formulation, they are also characterized by a fixed number of time-invariant friends. This is represented in Figure 3. In this setting, individual 23 is friend with 47 and 8, and individual 45 is friend with 54 and 36. Conditional on the heuristic, they both prefer to live close to their friends, who thus modifies their individual choices. Individual 23 will tend to move to get closer to 8 and 47. On the contrary, individual 45 will now tend to stay, since her friends live nearby. The effect of friends is therefore

non-monotonic as far the choice of moving is concerned, and generates a variable network externality on friends: for example, individuals 47 and 8 will tend to stay where they are after the move by 23.

The main elements of this reasoning are detailed, generalized and formalized in the subsequent model. For the sake of clarity, we proceed in a stepwise form.

3.1 | The framework

Consider a squared grid with side n, hence containing n^2 cells. We denote the set of the cells as V.

Each cell of the grid is identified by its row and column, so that $v_{rc} \in V$ is the cell at the intersection of row r and column c, for each $r, c = 1, \cdots, n$. For the sake of simplicity and when needed, we will call $v_{rc} = v$, where $v = (r - 1)n + c$. Such a definition of v labels with a real positive number all the elements of V, and it results that $v = 1, \cdots, n^2$. Hereafter, without loss of generality, we will use equivalently $v \in V$ and $v \in \{1, \cdots, n^2\}$.

To make every cell surrounded by an equal number of adjacent neighbors, we assume that the grid is suitably recombined at its boundary to be shaped as a torus, so that—for every $0 < h < n$ —each $v_{(n+h)c} = v_{hc}$ and $v_{r(n+h)} = v_{rh}$, for each $r, c, h = 1, \cdots, n$.

We introduce two different populations in the grid: the red individuals and the blue ones. For every individual, being blue or red is an immutable trait. The set collecting the reds and the blues are denoted by $\mathcal{A}$ and $\mathcal{B}$, with $|\mathcal{A}| = A$ and $|\mathcal{B}| = B$, respectively. We assume that the entire population belongs to the set $\mathcal{P} = \mathcal{A} \cup \mathcal{B}$. Each cell of the grid can be occupied by an element of $\mathcal{P}$ or it can be empty. Therefore, we have $A + B < n^2$. The generic elements of $\mathcal{A}$ and $\mathcal{B}$ will be denoted by a and b, respectively. We will refer to them as *agents*, and denote the generic agents as $i, j \in \mathcal{P}$.

All agents, also those sharing the same color, differ for the social connections they have. The social connections of agent i are represented by a star-shaped graph with i playing the role of the central hub. By merging together all the social connections of the agents in the grid, we have a unified graph composed by the individual $A + B$ (possibly interconnected) star-shaped subgraphs. We denote by $\mathbf{G} = (\mathcal{P}, E)$ the graph in the grid, where E represents the set of the edges of $\mathbf{G}$.

Specifically, we say that $(i, j) \in E$ if and only if there is a social connection between agent i and agent j, for each $i, j \in \mathcal{P}$. We define

$$\mathcal{P}_i := \{j \in \mathcal{P} | (i, j) \in E\}, \qquad \forall \, i \in \mathcal{P}.$$

The set $\mathcal{P}_i$ is the *friendship set* of the agent i, and $j \in \mathcal{P}_i$ is said to be *friend* of i. We assume that friendship disregards colors and thus, in general, $\mathcal{P}_i \cap \mathcal{A} \neq \emptyset$ and $\mathcal{P}_i \cap \mathcal{B} \neq \emptyset$, for each agent $i \in \mathcal{P}$.

Moreover, links are assumed to be undirected, so that $j \in \mathcal{P}_i$ if and only if $i \in \mathcal{P}_j$, for each $i, j \in \mathcal{P}$. At the same time, links are not weighted. Briefly, i and j are *friends*.

3.2 | Agents' preferences in the grid

Agents move in the grid, and their movement is driven by their level of satisfaction in occupying a given cell of the grid. Here, we discuss what are the criteria driving the preferences of an agent for a cell, while in the next subsections we will present agents' movement rule and the random assignment mechanism used to configure their initial position in the grid.

- *Color*. According to the classical Schelling model, we assume that agents prefer to be surrounded by people of the same color, and have a disutility in being surrounded by a majority of agents showing a color different from her own one. We formalize this assumption.

Given $\bar{r}, \bar{c} = 1, \cdots, n$ and the cell $\bar{v} = v_{\bar{r}\bar{c}} \in V$, we define the *neighborhood set of $\bar{v}$* by

$$N_{\bar{v}} := \{v_{rc} \in V \setminus \{\bar{v}\} \mid (r, c) \in \{\bar{r}-1, \bar{r}, \bar{r}+1\} \times \{\bar{c}-1, \bar{c}, \bar{c}+1\}\}. \tag{1}$$

By construction, we have that $|N_{\bar{v}}| = 8$. For each $\bar{v} \in V$, we introduce two variables $\xi_{\bar{v}}^A$ and $\xi_{\bar{v}}^B$ which describe the colors of $N_{\bar{v}}$ as follows:

$$\xi_{\bar{v}}^A := \frac{|N_{\bar{v}} \cap \mathcal{A}|}{8}, \qquad \xi_{\bar{v}}^B := \frac{|N_{\bar{v}} \cap \mathcal{B}|}{8}.$$

In general, $\xi_{\bar{v}}^A + \xi_{\bar{v}}^B \leq 1$.

For any agent $i \in \mathcal{P}$, the color-based normalized utility function of i in being located in the cells in V is $U_i^{color}: V \to [0, 1]$ such that $U_i^{color}(\bar{v})$ is not decreasing (not increasing, respectively) with respect to $\xi_{\bar{v}}^A$ when $i \in \mathcal{A}$ ($i \in \mathcal{B}$, respectively).

- *Friendship*. Agents prefer to locate close to their friends. To explain this extremely reasonable assumption, the introduction of a distance measure between couples of cells belonging to the squared grid is required. Without losing generality, we employ the normalized Manhattan distance $d: V^2 \to [0, 1]$ defined as

$$d(v_{r_1, c_1}, v_{r_2, c_2}) = \begin{cases} \dfrac{|r_1 - r_2| + |c_1 - c_2|}{n}, & \text{if } n \text{ is even}; \\ \dfrac{|r_1 - r_2| + |c_1 - c_2|}{n-1}, & \text{if } n \text{ is odd}. \end{cases} \tag{2}$$

where $r_1, r_2, c_1, c_2 = 1, \cdots, n$ and $v_{r_1, c_1}, v_{r_2, c_2} \in V$ and n in the normalizing factor.

With a reasonable abuse of notation, we will refer to $d(i, j)$ as the distance between two agents $i, j \in \mathcal{P}$, to be intended as the distance between the cells occupied by i and j and in accord to formula (2). In the same way, we will refer to $d(i, v)$ as the distance between the agent $i \in \mathcal{P}$ and the cell $v \in V$, which represents the distance between the cell occupied by i and the cell v. If agent i occupies the cell v, then $d(i, v) = 0$.

Notice that when i and j are friends, then $d(i, j)$ is the Manhattan distance between the cells representing the extremes of the edge (i, j). Moreover, by construction, $d(i, j) \in [0, 1]$.

Given an agent $i \in \mathcal{P}$, we can provide a measure of the friendship set $\mathcal{P}_i$. Clearly, such a measure depends on the specific cell $v \in V$ from which i's friends are observed. We denote such a measure as $\Delta(v, \mathcal{P}_i)$.

The measure Δ describes how an agent changes her closeness to her friends by modifying her position in the graph. As already mentioned above, we naturally assume that agent i, located in cell v, feels to be more satisfied about her connections (and surrounded by friendship) as the value of the $\Delta(v, \mathcal{P}_i)$'s is lower.[6]

---

[6]In the simulation in Section 4, we will provide a specific form of the Δ metric.

For any agent $i \in \mathcal{P}$, the friendship-based normalized utility function of i in being located in the cells in V is $U_i^{friend} : V \to [0, 1]$ such that $U_i^{friend}(v)$ is not increasing with respect to $\Delta(v, \mathcal{P}_i)$, for each $v \in V$.

- *Cost of moving.* Agents spend an effort in moving from a cell to another one, and such effort generates a disutility which does not decrease as the distance from the involved cells increases. Thus, for any agent $i \in \mathcal{P}$, the distance-based normalized utility function of i in moving from her position to the cells in V is $U_i^{moving} : V \to [0, 1]$ such that $U_i^{moving}(v)$ is not increasing with respect to $d(i, v)$, for each $v \in V$.

The utility function $U_i : V \to [0, 1]$—which drives the movement of the agents in the grid—is a convex combination of the utility functions described above, so that

$$U_i(v) := \alpha_c U_i^{color}(v) + \alpha_f U_i^{friend}(v) + \alpha_d U_i^{moving}(v), \tag{3}$$

where $\alpha_c, \alpha_f, \alpha_d \geq 0$ such that $\alpha_c + \alpha_f + \alpha_d = 1$. The selection of the values of the α's explains in a clear way the relevance of color, friendship, and movement effort in implementing the decision of moving from a cell to another one.

We stress that utilities have extreme zero (resp. unitary) value at the lowest possible (resp. highest possible) level of satisfaction. The range of the utility functions plays a key role here. In fact, the values of the utility function over the cells can be compared, and such comparison will drive the allocation procedure of the agents in the cells of the grid.

3.3 | The movement rule

The preferences described above represent the drivers of the movement of the agents in the grid. In this section, we describe how agents change their positions among the cells.

First, and without losing of generality, we assume that movements are on a sequential basis, that is the location process of the agents is with discrete time: that is, time $t \in \mathbb{N}$. The way in which agents move is straightforward: any moving agent changes her location cell with an empty one. In so doing, the graph **G** does not change, in the sense that friendships are constant over time. The component of the model which changes is represented by the set of the cells of the grid occupied by an agent and the empty ones. Given a time $t \in \mathbb{N}$, we denote the set collecting the empty cells at time t by Em_t and the set of the occupied ones by NEm_t, so that $V = Em_t \cup NEm_t$, for each $t \in \mathbb{N}$. By construction, $Em_t \cap NEm_t = \emptyset$.

We assume that only one agent moves each time.[7]

For a fixed time $t \in \mathbb{N}$, we denote the *configuration of the grid at time t by* $V_t = (EM_t, NEm_t)$. The agents start to move at time 1. Thus, V_t represents the situation of the grid at the t-th move— that is, after the moves of t agents—and identifies empty and occupied cells at time t.

We denote by *initial configuration* the grid at time $t = 0$, that is, V_0.

Of course, over time, the value of the utility functions of each agent in the cells of the grid may change. In fact, the passage from a configuration to another one is obtained by changing the position of one agent, and this might lead to a variation of the constitutive terms of the utility

---

[7]The extension to the case of simultaneous movements of agents can be, of course, presented. However, it does not add much to the single-moves case.

function U_i in (3) for some $i \in \mathcal{P}$. For any $i \in \mathcal{P}$ and $t \in \mathbb{N}$, we denote the utility function of agent i of being located in the cell v at time t as $U_i(v, t)$.

We are now in the position of describing the mechanism of the movement.

An agent moves only if the change of her position leads to an improvement of her utility. The first moving agent is the saddest one, that is, the one with the lowest level of utility of being located in her current position. The moving agent selects the empty cell which provides her/him the maximum level of utility.[8]

If more than one empty cell maximizes the utility, then the occupied one is randomly selected among the utility maximizing cells. Analogously, if more than one agent is in the position of moving, then the moving one is selected according to a uniform distribution over the available alternatives.

As an intuitive premise, we assume that any agent $i \in \mathcal{P}$ has a complete information at time t of the utility function $U_i(v, t)$, where v is the cell occupied by i at time t or $v \in Em_t$. Moreover, each agent is also aware about the peculiar distribution at time t of the agents belonging to $\mathcal{A}$ and $\mathcal{B}$. The agent moving at time t will be labeled as $j_t^\star$, whose definition is obtained according to the following two conditions:

$$
\begin{cases}
j_t^\star \in \text{argmin} \left\{ U_j(\bar{v}, t) \,|\, j \in \mathcal{P} \text{ located in } \bar{v} \in NEm_t \right\}; \\
\exists v \in Em_t \,|\, U_{j_t^\star}(v, t) \geq U_{j_t^\star}(\bar{v}, t)
\end{cases}
\tag{4}
$$

The two conditions in (4) must be jointly verified: the former one indicates that the moving agent is that with the lowest level of utility exerted from her position; the latter one specifies that the agent changes her position only if she will improve her utility.

The mechanism admits hypothetically simultaneous movements of different agents at time t, meaning that system (4) can be satisfied by more than one agent. By assuming that Q agents satisfy (4), with $Q = 1, \cdots, A + B$, we will label the Q moving agents by $j_{1,t}^\star, \cdots, j_{q,t}^\star, \cdots, j_{Q,t}^\star$. A random extraction of one element of the set $\{1, \cdots, Q\}$ identifies univocally $\bar{q} \in \{1, \cdots, Q\}$ such that the moving agent is $j_t^\star = j_{\bar{q},t}^\star$.

Once condition (4) is satisfied and the moving agent identified, we implement the selection of the empty cell where agent $j_t^\star$ moves. As already mentioned above, this selection is driven by the agent's utility function. We model the utility of an agent to move to an empty cell $v_t^\star$ as follows:

$$
v_t^\star \in \Phi_t := \text{argmax} \left\{ U_{j_t^\star}(v, t) \,|\, v \in Em_t \text{ and } U_{j_t^\star}(v_{t-1}, t) < U_{j_t^\star}(v, t) \right\},
\tag{5}
$$

with the conventional agreement that $v_t^\star = v_{t-1}$ if $\Phi_t = \emptyset$.

If $|\Phi_t| = C > 1$, then there are C different cells in Em_t which are indifferent—in terms of the utility function—for the moving agent $j_t^\star$. We will label such C utility maximizer cells by $v_{1,t}^\star, \cdots, v_{c,t}^\star, \cdots, v_{C,t}^\star$. In this case, we extract randomly one element of the set $\{1, \cdots, C\}$, and identify accordingly $\bar{c} \in \{1, \cdots, C\}$ such that the selected empty cell is $v_t^\star = v_{\bar{c},t}^\star$.

---

[8]A movement rule where, at each stage, one agent is randomly selected and asked to choose a best-response was previously used by Pancs and Vriend (2007).

The movement of $j_t^\star$ induces a new configuration of the grid, which passes from V_{t-1} to V_t. The movement process then continues according to this mechanism. A new moving agent $j_{t+1}^\star$ is identified, which changes her original position with the empty cell $v_{t+1}^\star$.

The process stops at the first time in which all the agents cannot improve their utility when moving from their position to an empty cell. Clearly, the process can also never stop. For this reason, in the numerical experiments we will stop the process also in presence of loops, that is, in the circumstance of an agent moving iteratively back and forth between two cells.

4 | SIMULATION

The dimensionality of the problem requires the model to be solved by simulation (Axelrod, 2013; Velupillai & Zambelli, 2015). The basic elements of the model, described in Section 3, are articulated through computation[9] and mimic a process that, given basic exogenous conditions (i.e., the spatial dimension, the density of agents, the relative share of the two populations) and the social context (Akerlof & Kranton, 2000), begin with agents' moving choices and ends to the determination of stable equilibria, corresponding to a certain level of individual and social utility and of racial residential segregation. The simulation procedure can be seen as the numerical analogous to an experimental procedure (Bona & Santos, 1997), where the parameters of the model are shocked to check the response of the system and evaluate the resulting levels of utility and segregation.

In this section, we details the main aspects of our simulation setup.

4.1 | Generating starting positions and network connections

We consider an $n \times n$ torus with $n = 10$, and impose that $A = B = 37$, and 26 cells are left empty. Agents' initial configurations are established at random.[10] In order to avoid spurious results, the initial configurations $V_0^{(h)}$ is permuted H times by using just as many random seeds, so that the hth seed generates the hth initial configuration of the grid $V_0^{(h)}$, with $h = 1, \cdots, H$. We set $H = 100$, to get a distribution of results. The moments of said distribution are then summarized and plotted systematically.

Next, we create the graph **G**. For consistency with the literature of social networks (Barabási, 2016; Goyal, 2009; Jackson, 2010; Newman, 2010) for applications to economics), we denote by $k = 0, 1, \cdots, 73$ the degree centrality of each node, which in this case it is assumed to be fixed, that is, we assume a common degree k for the hub of the star-shaped subgraphs. By considering the random seed of initial configuration, h and the degree k, we define $\mathbf{G} := \mathbf{G}_{h,k} = (\mathcal{P}, E_{h,k})$ as composition of the regular star-shaped graphs for the agents in $\mathcal{P}$. Clearly, the cardinality of the set of arcs $E_{h,k}$ depends on k, so that, for example, graph $\mathbf{G}_{h,2}(m)$ will have 74×2 arcs, and all the agents will have degree centrality equal to 2—that is, each agent has two friends. For the sake of simplicity, and without loss of generality, we assume that $E_{h,k_1} \subset E_{h,k_2}$ with $k_1 < k_2$: that is, an arc in a

---

[9]All computation is programmed in R and is available upon request for replication purposes.

[10]This implies that agents are positioned in the torus without following any specific pattern (e.g., a situation of integration or segregation). Instead, they are seamlessly located next to one another.

graph $\mathbf{G}_{h,k_1}$ is also an arc in $\mathbf{G}_{h,k_2}$. Consequently, $\mathbf{G}_{h,k_1}$ can be regarded as a subgraph of $\mathbf{G}_{h,k_2}$ when $k_1 < k_2$.

4.2 | The utility function

We now introduce the functional form of formula (3) assumed by the simulations.

To this purpose, we begin with the component of agent's utility exerted from their location, U^{color}. We introduce a prespecified threshold $x \in (0,1)$ which drives Schelling's heuristic. We label x as *Schelling's threshold*. Specifically, x determines the maximum density of same-color neighbors required by i to be satisfied by her residential location, so that

$$U_i^{color}(\overline{v}) = U_i^{color}(\overline{v};x) = \begin{cases} \xi_{\overline{v}}^A \cdot 1_{\{\xi_{\overline{v}}^A > x\}}, & \text{if } i \in \mathcal{A}; \\ \xi_{\overline{v}}^B \cdot 1_{\{\xi_{\overline{v}}^B > x\}}, & \text{if } i \in \mathcal{B}; \end{cases} \tag{6}$$

for each $\overline{v} \in V$ and $1_{\bullet}$ is the indicator function of the set $\bullet$. Formula (6) gives that when $x = 0$, i is "color-blind" and does not benefit from any change of location when looking at the color of the surrounding agents. By contrast, when $x = 1$, i will enjoy any marginal increase in the number of same-color neighbors.

Next, we define the utility obtained from friendship, U^{friend}, as:

$$U_i^{friend}(\overline{v}) = 1 - \Delta(\overline{v}, \mathcal{P}_i), \tag{7}$$

where $\Delta(\overline{v}, \mathcal{P}_i)$ is the average Manhattan distance in (2) between i and her friends, that is:

$$\Delta(\overline{v}, \mathcal{P}_i) = \frac{1}{k} \sum_{j \in \mathcal{P}_i} d(i, \overline{v}). \tag{8}$$

Then, we formalize the cost of moving, U^{moving}, as:

$$U_i^{moving}(\overline{v}) = 1 - [\gamma \overline{c} + (1 - \gamma)(1 - \overline{c})(1 - d(i, \overline{v}))] \tag{9}$$

where $\overline{c} \in (0,1)$ is the cost of moving between two adjacent cells and $\gamma \in \{0,1\}$ determines whether costs are fixed ($\gamma = 1$) or variable ($\gamma = 0$).

Finally, we turn to the responsiveness of i's utility to a change in U_{color}, U_{friend} and U_{moving}, and we set:

$$\begin{aligned} \alpha_c &= \beta\alpha \\ \alpha_f &= \beta(1-\alpha) \\ \alpha_d &= 1-\beta \end{aligned} \tag{10}$$

where $\alpha \in [0,1]$ and $\beta \in [0,1]$.

As a result, we can re-write formula (3) by using (6)–(10) and explicitating the Schelling's threshold x of the utility dependent on the color as follows:

$$U_i(\overline{v}) = U_i(\overline{v};x) = \beta(\alpha U_i^{color}(\overline{v};x) + (1-\alpha)U_i^{friend}(\overline{v})) + (1-\beta)U_i^{moving}(\overline{v}). \tag{11}$$

4.3 | Measures of segregation

Measuring the level of segregation adds an additional layer of complexity to our analysis. The level of agents' dissimilarity in a location is traditionally studied at the neighborhood level, where the boundaries of the residential area are exogenously defined (Massey & Denton, 1988). By contrast, here we are interested in the agent's level of segregation, which is endogenously determined by the agent's own location. For this reason, we prefer over standard metrics of segregation (Massey & Denton, 1988), the measurement provided by the Freeman Segregation Index (*FSI*) (Bojanowski & Corten, 2014; Freeman, 1978), and the Moran's *I* index (Moran, 1950), which allow to assess the degree to which individuals with similar attributes are located close to one another when the neighborhood is self-referenced.

Fagiolo et al. (2007) and Mele (2017) show that *FSI* can be profitably used to study agents' contiguity in a grid-like topological space, such as a torus, by using a graph perspective. Consistent with this approach and according to the model outlined above, we consider two groups of agents—the red and the blue ones—whose cardinalities are A and B, respectively, and label all the agents with an integer $i = 1, \cdots, A + B$. We consider the friendship graph $\mathbf{G}$ and introduce its randomized version $\mathbf{G}_h$, where $h = 1, \cdots, H$ is the seed, as follows: agents represent the nodes and the generic entry $w_{i,j}^{(h)}$ of the symmetric adjacency matrix W_h is 1 when the two agents i and j are adjacent in the grid—according to formula (1)—and 0 otherwise. The maximum number of arcs $\overline{N}_E$ in $\mathbf{G}_h$ does not depend on h and is given by:

$$\overline{N}_E = \binom{A+B}{2} = \frac{(A+B)(A+B-1)}{2},$$

while the maximum number of cross-group arcs is AB.

Consequently, if agents are "color blind" and arcs are generated independently of each other, the probability of a given arc being a cross-group arc is:

$$p = \frac{AB}{\overline{N}_E} = \frac{2AB}{(A+B)(A+B-1)}$$

As a consequence, given the number of arcs in $\mathbf{G}$, say N_E, the expected number of cross-group arcs is $E(N_E^*)$ defined as follows:

$$E(N_E^*) = N_E p$$

Given this formalization, *FSI* is obtained as:

$$FSI = \operatorname{argmax}\left\{ 0, \frac{E(N_E^*) - N_E^c}{E(N_E^*)} \right\}, \tag{12}$$

where N_E^c is the observed number of cross-group arcs. *FSI* varies between 0 and 1, and it may be interpreted as the proportion by which the expected number of cross-group links is reduced in observation. Specifically, a value of 0 indicates full integration, while a value of 1 corresponds to full segregation. Put differently, when $FSI = 1$, there is a positive autocorrelation in the spatial distribution of agents: that is, blue and red nodes are located in different and non-contiguous areas. On the

contrary, when $FSI = 0$, there is no autocorrelation present, that is, blue and red nodes are distributed at random in the torus.

We complement the FSI, with the Moran's I index, which is calculated as:

$$I = \left(\frac{A+B}{\sum_{i=1}^{A+B} \sum_{j=1}^{A+B} w_{i,j}} \right) \left(\frac{\sum_{i=1}^{A+B} \sum_{j=1}^{A+B} w_{i,j}(z_i - \overline{z})(z_j - \overline{z})}{\sum_{i=1}^{A+B} (z_i - \overline{z})^2} \right) \tag{13}$$

where z_i is equal to 1 if i is red, and 0 if i is blue, and $\overline{z} = \frac{\sum_{i=1}^{A+B} z_i}{A+B}$. The values of the Moran's I range in the interval $[-1, 1]$. When $I = -1$, then one has the maximum possible negative spatial autocorrelation: for example, red agents are adjacent only to blue agents. When $I = 1$, there is the maximum level of positive spatial autocorrelation: for example, each red agent is surrounded by red agents.

It is interesting to note that FSI and Moran's I are both correlated with another well-known index, that is Geary (1954)'s metrics G, a measure of spatial autocorrelation which goes from 0 (maximum level of positive autocorrelation) to 2 (maximum level of negative autocorrelation). Specifically, G is equal to the reciprocal of FSI, when $G \in (0, 1)$ (Freeman, 1978), and it is inversely correlated with I (Anselin, 1995). By virtue of this, FSI and Moran's I are positively correlated when $I \geq 0$. However, they are not identical. The former is more sensitive to local patterns of segregation, while the latter is better suited for detecting segregation at the global level. The reason is that FSI mimics the measurement of G, and Anselin (1995) has shown that G is more susceptible than I to local structures of segregation. We expect this difference to be preserved also when comparing FSI and I.

5 | SIMULATION EXPERIMENTS, RESULTS, AND DISCUSSION

This section presents the simulation experiments, and discuss the results of our investigation. In order to disentangle the effect exerted by the different components of the utility function, as formalized in formula (11), a stepwise approach is adopted. First, we test plain Schelling's model, without moving costs and friendship connections. Next, we include the presence of moving costs, and then the presence of agents' connections. Finally, we present the case of Schelling's model and friendship, without moving costs, and in the extreme case of maximum Schelling's threshold $x = 1$.

The results of the simulation are assessed by looking at six different outcomes: (i) the number of iterations required by the model in order to converge and produce the final configuration; (ii) the number of agents who are affected by the process in motion and leave their initial position during the iteration process; (iii) the FSI and (iv) the Moran's I index of the torus when model convergence is reached; (v) the average and the (vi) total social welfare of the agents at the end of the iteration process. Formally, (v) and (vi) are the average and the sum of individual agents' utilities in the final configuration of the torus, as obtained from formula (11). For each model setting, we report the second, the third, and the fourth quintile of these metrics obtained in H different random initial configurations of the torus.
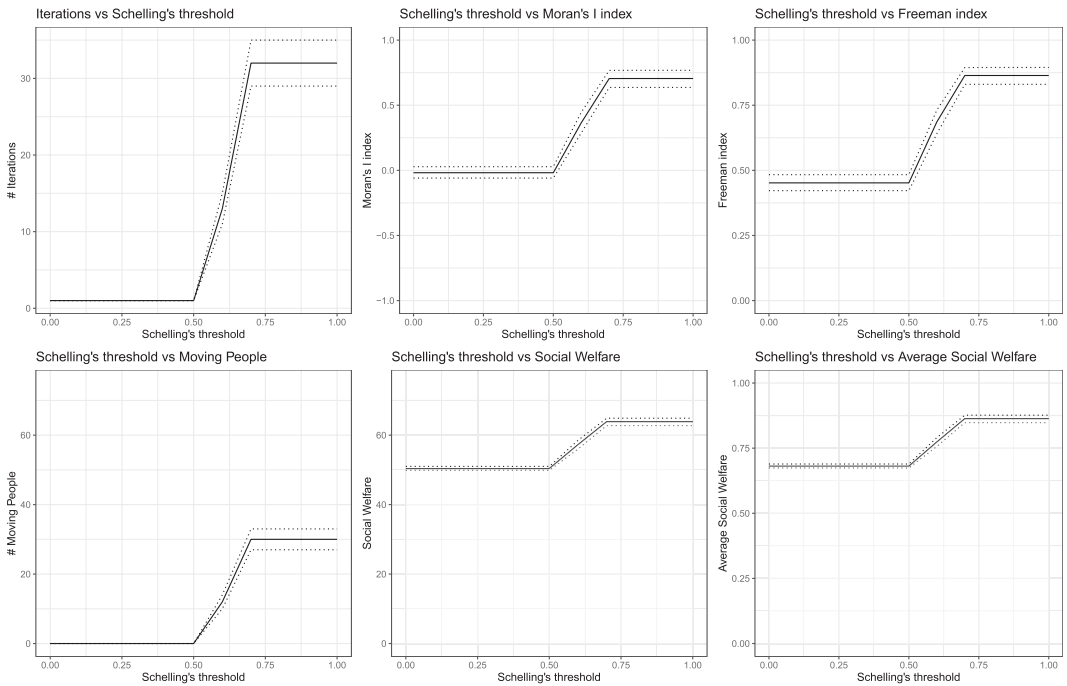
FIGURE 4 No Moving costs ($\beta = 1$)—No contribution of friendship to utility ($\alpha = 1$). Each simulation is repeated $H = 10,000$ times by permuting the initial torus. On the abscesses, the Schelling's threshold x ranging in $[0, 1]$. Lines indicate, respectively, the second (lower ticked line), the third (bold line), and the fourth (upper ticked line) quintile of the distribution of values obtained. Upper left panel indicates the number of iterations required for the model to converge for different x values. Upper middle and right panels report, respectively, the Moran's I and the FSI value obtained after model convergence. Bottom left panel shows the number of people who moved at least once in a simulation. Bottom middle and right panels display, respectively, the average and the total social welfare of the agents at the end of the iteration process. Social welfare is obtained from the component $\beta\alpha U_i^{color}(\overline{v};x)$ of the i-th agent utility function (Equation 11)

5.1 | Schelling's model

In this first array of experiments, moving costs and friendships are sorted out from the definition of the utility function in (11), i.e. $\beta = \alpha = 1$. The analysis is focused on agents' responsiveness to the variation of the Schelling's threshold x.

This first simulation experiment sets the baseline to evaluate the other results. Results are shown in Figure 4, which illustrates the change in each outcome (on the y-axes) for increasing levels of the Schelling's threshold x.

Model results are straightforward and consistent with the original Schelling model. When $x = 0$ (and, we stress it, agents assign no value to social connections: that is, $\alpha = 1$), homophily play no rule in agents' relocation choices. Agents are indifferent to the density of same-color people in the neighborhood, and they have no incentives to move. As a result, the initial configuration remains unchanged and social welfare is unaltered. By contrast, when there is a preference for neighborhoods characterized by a majority of same-color agents, that is, $x \geq 0.5$, people begin to move, increasing the level of both segregation and social welfare. Specifically, we observe that when $x > 0.7$, total segregation is almost reached, and approximately 50% of the population is
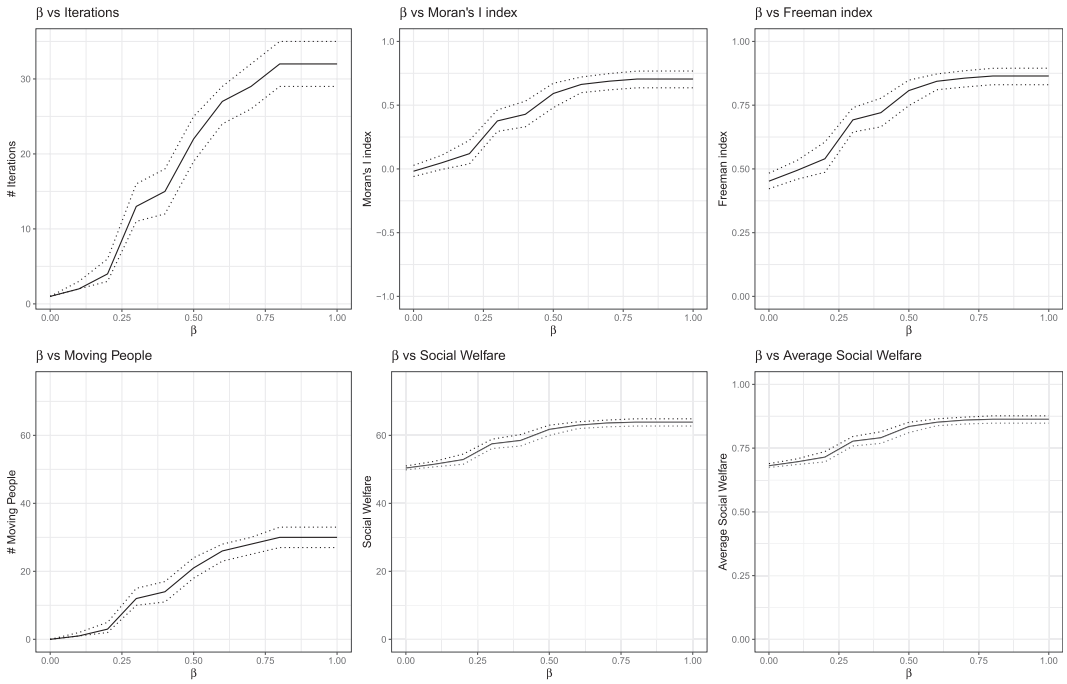
FIGURE 5 Fixed moving costs ($\gamma = 1$, $\bar{c} = 0.5$)—Maximum value of the Schelling's threshold $x = 1$—No contribution of friendship to utility ($\alpha = 1$). On the abscesses, the parameter β ranging in [0, 1]. Each simulation is repeated $H = 10{,}000$ times by permuting the initial torus. Lines indicate, respectively, the second (lower ticked line), the third (bold line), and the fourth (upper ticked line) quintile of the distribution of values obtained. Upper left panel indicates the number of iterations required for the model to converge. Upper middle and right panels report, respectively, the Moran's I and the FSI value obtained after model convergence. Bottom left panel shows the number of people who moved at least once in a simulation. Bottom middle and right panels display, respectively, the average and the total social welfare of the agents at the end of the iteration process. Social welfare is obtained from the component $\beta \alpha U_i^{color}(\bar{v};x)$ of i-th agent's utility function (Equation 11)

involved in a change of location, implying that our model is able to describe large population movements.

5.2 | Schelling's model with moving costs

The role played by moving costs is to affect agents' location choices by mitigating the attraction force determined by their preference over homophily. In particular, this component of the agent's utility function discourages long movements and contrast the emergence of complete segregation. In order to show this effect, we simulate how the model initial configuration is changed for different levels of agents' responsiveness to either fixed or variable moving costs, that is, with respect to β in [0, 1]. Specifically, we set $x = 1$, $\alpha = 1$, $\bar{c} = 0.5$ and the two extreme scenarios $\gamma = 0$ and $\gamma = 1$. The results of this exercise are presented, respectively, in Figure 5, where we impose a fixed cost on agents' moves, and in Figure 6, where we allow agent's moving costs to be variable. In both figures, the plots show the effect of a change in β, displayed on the x-axes, on one of the six outcomes considered, reported on the y-axis.
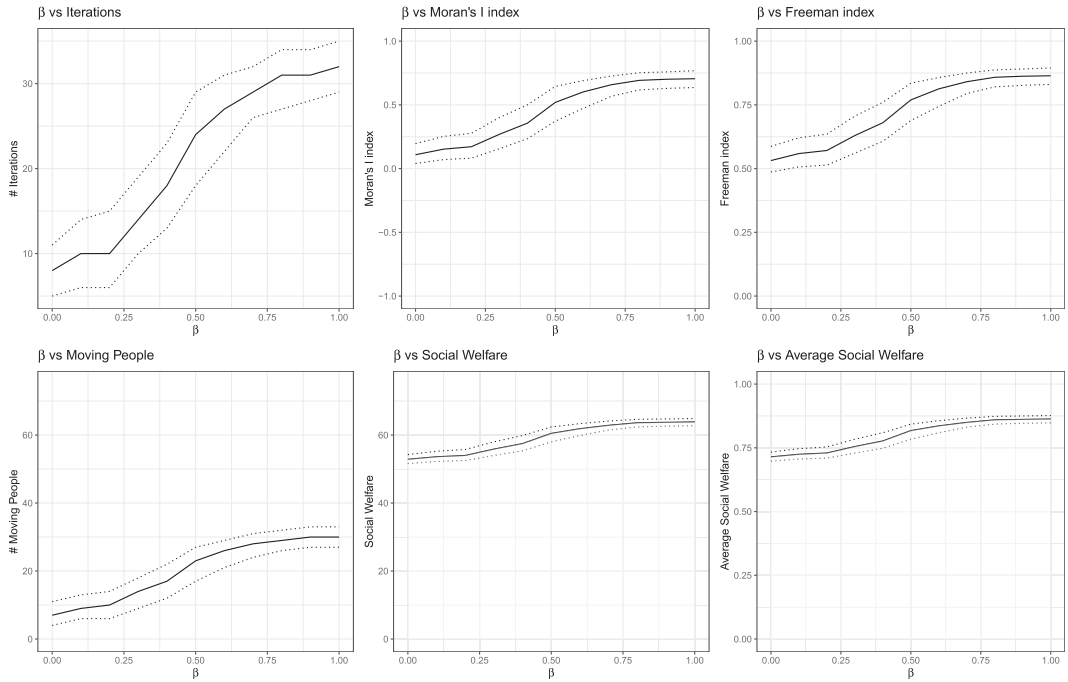
FIGURE 6 Variable moving costs ($\gamma = 0$, $\bar{c} = 0.5$)—Maximum value of the Schelling's threshold $x = 1$—No contribution of friendship to utility ($\alpha = 1$). On the abscesses, the parameter β ranging in [0, 1]. Each simulation is repeated $H = 10,000$ times by permuting the initial torus. Lines indicate, respectively, the second (lower ticked line), the third (bold line), and the fourth (upper ticked line) quintile of the distribution of values obtained. Upper left panel indicates the number of iterations required for the model to converge. Upper middle and right panels report, respectively, the Moran's I and the FSI value obtained after model convergence. Bottom left panel shows the number of people who moved at least once in a simulation. Bottom middle and right panels display, respectively, the average and the total social welfare of the agents at the end of the iteration process. Social welfare is obtained from the component $\beta \alpha U_i^{color}(\bar{v};x)$ of i-th agent's utility function (Equation 11)

Consistent with expectations, the results show a monotonic relation between agents' responsiveness and the number of individual movements: that is, the lower the moving costs, the higher is the number agents changing their location (bottom-left plots). Analogously, when moving costs decreases, the number of model iterations (i.e., the number of steps before convergence) increases, and convergence timing is delayed (top-left plots).

In addition, we see that when agents are left free to relocate (i.e., β decreases), the model tends to mimic Schelling's results: that is, blue and red nodes move in different and non-contiguous areas, and segregation increases in terms of both *FSI* and Moran's I values (top-middle and right panel). This is not surprising, since network effects are null (i.e., degree centrality is equal to 0), and Schelling's heuristic is the only determinant of movements.

Finally, we witness a negative relation between moving costs and social welfare (bottom-middle and right panel). Specifically, the highest levels of agents satisfaction are reached when $\beta \geq 0.75$. Above this value, $U_i(\bar{v})$ remains somewhat constant.

The robustness of these results is confirmed by further analyses presented in the Appendices, where we show that results are left qualitatively unchanged when replicating this exercise using low fixed costs (Figure A1, with $\gamma = 1$ and $\bar{c} = 0.01$), low variable costs (Figure A2, with $\gamma = 0$ and

$\bar{c} = 0.01$), high fixed costs (Figure B1, with $\gamma = 1$ and $\bar{c} = 0.99$), and high variable costs (Figure B2, with $\gamma = 1$ and $\bar{c} = 0.99$).

5.3 | Schelling's model with moving costs and networked individuals

In the third experiment, we test the different effects between having no friends, or having some friends, while moving costs are at work. To this purpose, we set agents' degree centrality k equals to 3, and we test the scenarios for $\alpha = 1$ (utility does not depend on friendship) and $\alpha = 0.5$ (agents assign equal weights to neighborhood composition and friends' distance), while fixing the value of the parameters relative to moving costs (β and γ) to a constant (and positive) value to make a correct comparison. Specifically, the value of β is set to 0.5, to represent a fair introduction of the moving costs in the utility. The impact of this parameter on the model outcome is alternatively tested by setting $\gamma = 0$ (i.e., fixed costs) and $\gamma = 1$ (i.e., variable costs). Moreover, we also investigate changes in the model outcome when moving costs are removed by taking $\beta = 1$. The simulation experiments are performed by taking into account the sensitivity with respect to Schelling's threshold x.

We first refer to results in Figure 7. The introduction of the friendship network has a dramatic impact on the results. The force of attractiveness generated by the homophily preferences is now bonded by the different characteristics with which agents identify (i.e., the color and the social connection). Moreover, agents' movements are constrained by the tension exerted by friends' position, who are in turn attracted by their friends. We first focus on this latter element. When neighborhood composition is irrelevant, that is, $x = 0$, friendship drives homophily and generates two competing forces. The first is an attractive force, like a spring, which brings agents that are linked closer together. The second is a repulsive force, generated by the presence of multiple connections, which prevents long movements of people to the same area, and forces friends apart from each other. Put differently, network externalities are at play, and their effects cascade quite dramatically. As a result, agents act as if they were steel rings linked by springs, and any radical change in the original status quo is prevented: that is, less than 25% of the population choose to change location and model convergence is reached with few iterations. It follows that total segregation is far from being reached in this setting.

However, when agents begin to care about the characteristics of their neighbors, $x > 0$, a significant change occurs on their preferences over the composition of their neighbors. This results in a reduction of the local inertia determined by network externalities, and the set of individual relocation choices expands. This produces an increase of both segregation and social welfare, but interestingly, both outcomes remain significantly lower than those achieved in Figure 4, meaning that the introduction of the network has the simultaneous effect of reducing segregation and producing suboptimal levels of welfare.

This finding provides an interesting insight. When homophily requires to combine multiple characteristics, agents find it difficult to find a neighborhood that improves her levels of welfare: for example, a racially mixed neighborhood where the majority is composed by people of her own color, and the minority is represented by her social connections.

When we set $\beta = 0.5$, then we observe a contribution to our analysis, regardless of whether we consider network effects or not. In fact, significant changes are registered neither when costs are fixed (Figures 8 and 9) nor when costs are variable (Figures 10 and 11), and results remain
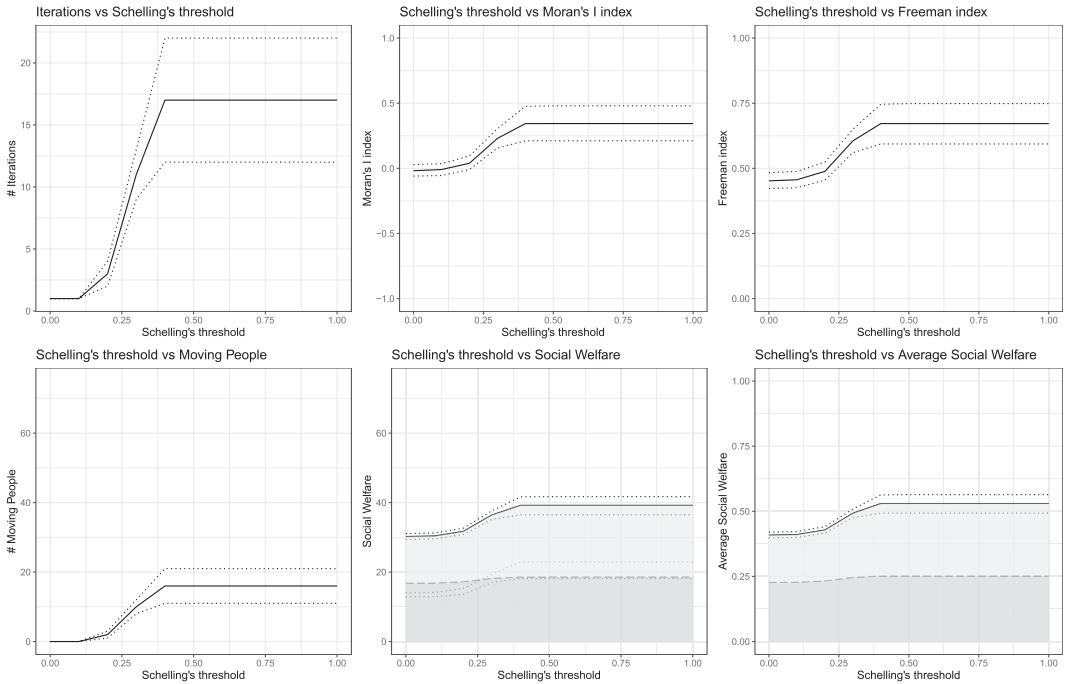
FIGURE 7 No Moving costs ($\beta = 1$)—fair utility from friendship and Schelling's heuristics ($\alpha = 0.5$)—3 friends ($k = 3$) Each simulation is repeated $H = 10,000$ times by permuting the initial torus and network connections. On the abscesses, the Schelling's threshold x ranging in [0, 1]. Lines indicate, respectively, the second (lower ticked line), the third (bold line), and the fourth (upper ticked line) quintile of the distribution of values obtained. Upper left panel indicates the number of iterations required for the model to converge. Upper middle and right panels report, respectively, the Moran's I and the FSI value obtained after model convergence. Bottom left panel shows the number of people who moved at least once in a simulation. Bottom middle and right panels display, respectively, the average and the total social welfare of the agents at the end of the iteration process. Social welfare is obtained from i-th agent's utility function (Equation 11). The color of the area indicates the two components of agent's utility after convergence is achieved: $\beta\alpha U_i^{color}(\overline{v};x)$ (lighter-colored area) and $\beta\alpha U_i^{friend}(\overline{v})$ (darker-colored area)

qualitatively the same.[11] All in all, the introduction of moving costs only produces a shift in the outcomes value.

The only difference found is when we consider the combination of high fixed moving costs and no friends ($\gamma = 1, \alpha = 1$ and $\overline{c} = 0.99$, see Figure B3). In fact, in this case there is no incentive to move, convergence is achieved after one iteration and the original status quo remains unchanged. In other words, we observe a different mechanism for the configuration of a system of local inertia, where the effect of homophily is nullified by moving costs. It should not be surprising that the same does not apply to the case of variable costs ($\gamma = 0, \alpha = 1$ and $\overline{c} = 0.99$, see Figure B5). While in the former case any movement has the same cost, in the latter setting the cost of changing location is mitigated by distance, and short movements are still possible.

---

[11]Additional evidence is reported in Figure 7, where we test the effect of reducing fixed costs ($\gamma = 1$ and $\overline{c} = 0.01$, see Figures A3 and A4) and variable costs ($\gamma = 0$ and $\overline{c} = 0.01$, see Figures A5 and A6). Similarly, in 8, we test the effect of increasing fixed costs ($\gamma = 1$ and $\overline{c} = 0.99$, see Figures B3 and B4) and variable costs ($\gamma = 1$ and $\overline{c} = 0.99$, see Figures B5 and B6).
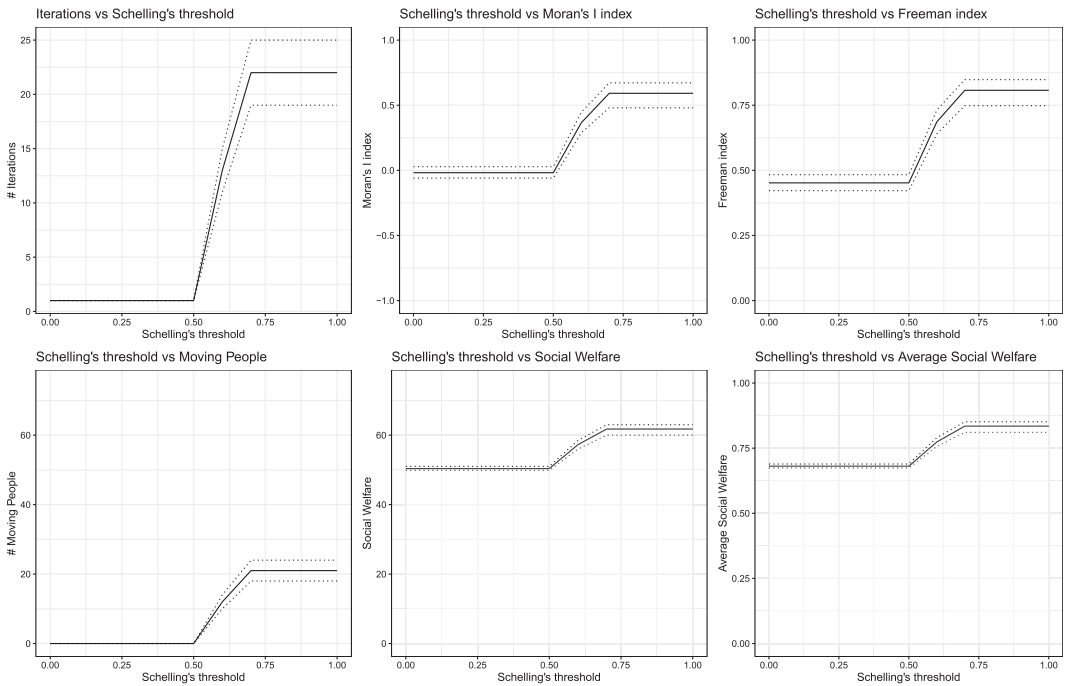
FIGURE 8 Fixed moving costs ($\beta = 0.5$, $\gamma = 1$, $\bar{c} = 0.5$)—No contribution of friendship to utility ($\alpha = 1$). Each simulation is repeated $H = 10{,}000$ times by permuting the initial torus. On the abscesses, the Schelling's threshold x ranging in [0, 1]. Lines indicate, respectively, the second (lower ticked line), the third (bold line), and the fourth (upper ticked line) quintile of the distribution of values obtained. Upper left panel indicates the number of iterations required for the model to converge. Upper middle and right panels report, respectively, the Moran's I and the FSI value obtained after model convergence. Bottom left panel shows the number of people who moved at least once in a simulation. Bottom middle and right panels display, respectively, the average and the total social welfare of the agents at the end of the iteration process. Social welfare is obtained from ith agent's utility function (Equation 11)

5.4 | An extreme case of Schelling's model and the networked individuals

The effect of the network on agents' location choice when neighborhoods composition matters is further investigated in this section. In the experiment summarized in Figure 12, Schelling's threshold is stressed by setting x equals to 1, meaning that agents are sensitive to any marginal change in their neighborhood composition. Moving costs are removed, by taking $\beta = 1$, while $\alpha = 0.5$, which means that there is a fair contribution of Schelling's heuristics and friendships. Degree centrality k is let to vary iteratively, from 0 to 73. Therefore, now the abscesses of the plots reports the level of degree centrality, while the y-axes are used once again to register changes in the outcome values. For illustrative purposes, Figure 13 shows also various instances of the final torus configuration when increasing degree centrality.

As expected, when degree centrality is 0, the model replicates the last observation registered in the plots of Figure 4. Then, when agents form a friendship, a significant change occurs in the formation of individual homophily preferences. As a result, the utility exerted from positioning close to an agent is now equivalent to the utility obtained by locating in a neighborhood where all agents have the same color. In other words, we observe the configuration of a peculiar physical
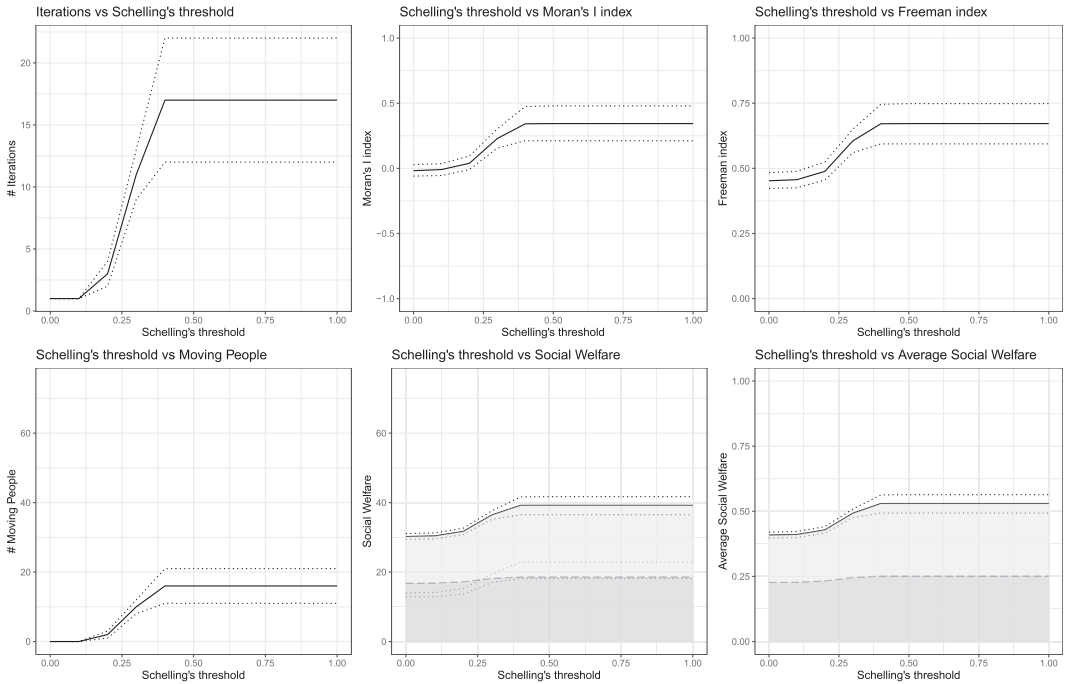
FIGURE 9 Fixed moving costs ($\beta = 0.5$, $\gamma = 1$, $\bar{c} = 0.5$)—Fair utility from friendship and Schelling's heuristics ($\alpha = 0.5$)—3 friends ($k = 3$). Each simulation is repeated $H = 10{,}000$ times by permuting the initial torus. On the abscesses, the Schelling's threshold x ranging in $[0, 1]$. Lines indicate, respectively, the second (lower ticked line), the third (bold line), and the fourth (upper ticked line) quintile of the distribution of values obtained. Upper left panel indicates the number of iterations required for the model to converge. Upper middle and right panels report, respectively, the Moran's I and the FSI value obtained after model convergence. Bottom left panel shows the number of people who moved at least once in a simulation. Bottom middle and right panels display, respectively, the average and the total social welfare of the agents at the end of the iteration process. Social welfare is obtained from i-th agent's utility function (Equation 11). The color of the area indicates the two components of agents' utility after convergence is achieved: $\beta\alpha U_i^{color}(\bar{v};x)$ (lighter-colored area) and $\beta\alpha U_i^{friend}(\bar{v})$ (darker-colored area)

system unconstrained by the repulsive forces generated by the composition of the neighborhood or by multiple friendships. If agents choose a location close to their friend, this in turn has no need to relocate. Consequently, the utility obtained by the composition of the neighborhood suddenly drops, and we observe a significant decrease in the segregation indices.

The externalities produced by the combination of Schelling's heuristic and social linkages are an important component of our model, because they show how competing identities modify homophily effects. As agents reach a neighborhood, others who are in the neighborhood might decide to remain regardless of their color, and the composition of their neighbors. This mechanism generates limited segregation equilibria and suggests an explanation for the existence of racially mixed neighborhoods. This is somewhat the case described in the upper-right panel in Figure 13: agents 69 and 79 are friends living in adjacent cells, so even if the latter does not enjoy the composition of the neighborhood, they decide not to move. A similar behavior is observed for agents 18 and 36. Since 36 benefits from the new composition of the neighborhood, and she has not incentives to move, 18 decides to remain in the starting position, which is relatively close to 36, even if no blue agents are in the surroundings.
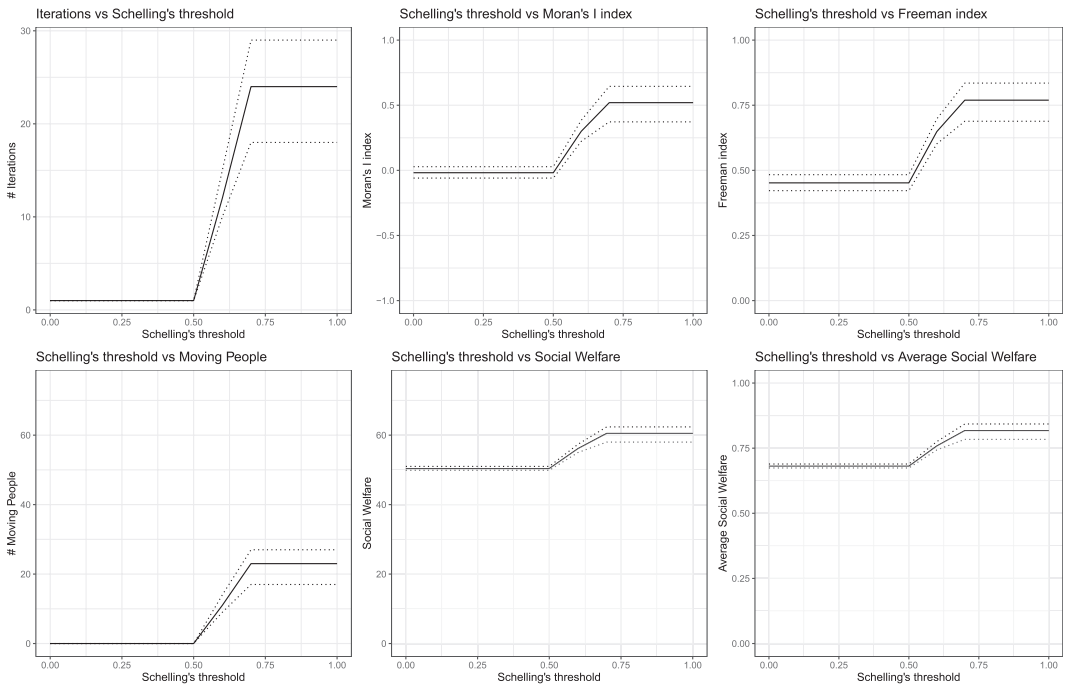
FIGURE 10   Variable moving costs ($\beta = 0.5$, $\gamma = 0$, $\bar{c} = 0.5$)—No contribution of friendship to utility ($\alpha = 1$). Each simulation is repeated $H = 10{,}000$ times by permuting the initial torus. On the abscesses, the Schelling's threshold x ranging in $[0, 1]$. Lines indicate, respectively, the second (lower ticked line), the third (bold line), and the fourth (upper ticked line) quintile of the distribution of values obtained. Upper left panel indicates the number of iterations required for the model to converge. Upper middle and right panels report, respectively, the Moran's I and the FSI value obtained after model convergence. Bottom left panel shows the number of people who moved at least once in a simulation. Bottom middle and right panels display, respectively, the average and the total social welfare of the agents at the end of the iteration process. Social welfare is obtained from i-th agent's utility function (Equation 11)

However, when k increases, agents begin to look for an equilibrium in between the distance from their friends and the neighborhood where they live in. In this attempt to manage multiple preferences, agents seem to give more importance to the composition of their neighborhood than to their friends location, since the utility obtained by the former factor increases, while the latter decreases. This might be due to the fact that agents find easier to locate in a neighborhood with specific characteristics and close to few friends, than finding a place that is suitable for all her friends. This is for example the case of agents 9 and 36, in the middle-left panel of Figure 13. Both of them are relatively close to one of their friends, and located in a neighborhood where all agents share her own color.

This is another important finding of this study. Competing characteristics do not equally matter in forming agents homophily preferences. Rather, certain characteristics featured by the agent tend to prevail in the definition of her own identity because it is easier to locate close to someone with that same characteristics (e.g., color over social linkages). Hence, even when agents assign the same importance to all their characteristics (e.g., $\alpha = 0.5$), some of them will have a stronger impact on relocation choices.

This mechanism is even clearer if we consider the case where each individual is connected with more than a relatively small proportion of the population (ca. 5%–8%). In fact, when the
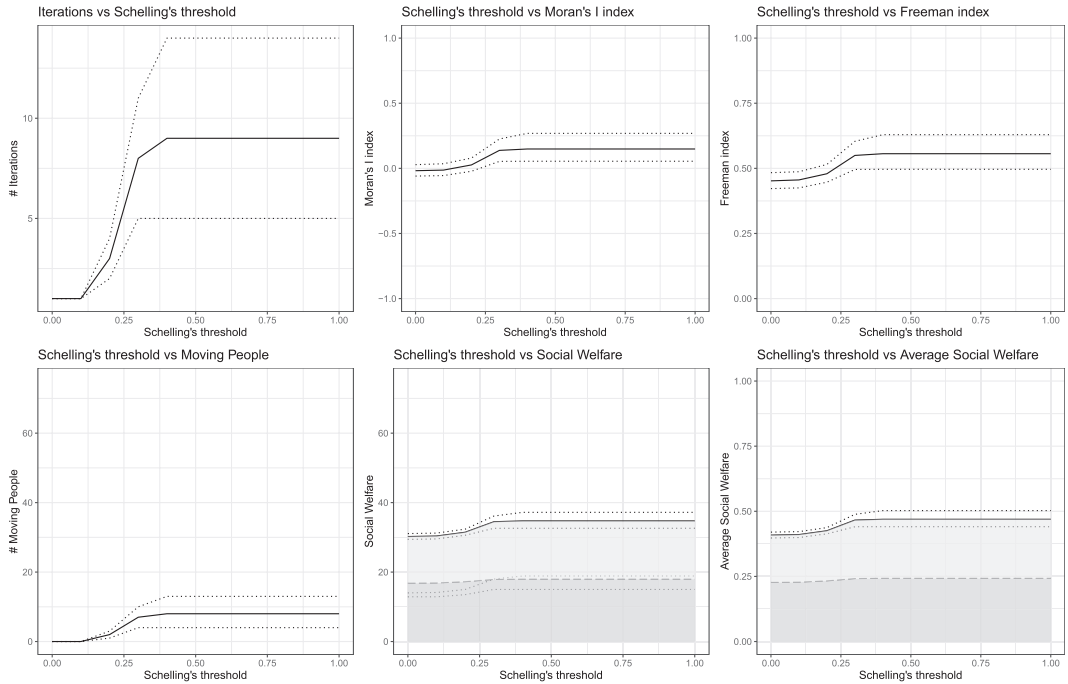
FIGURE 11 Variable moving costs ($\beta = 0.5$, $\gamma = 0$, $\bar{c} = 0.5$)—Fair utility from friendship and 3 friends ($\alpha = 0.5$, $k = 3$). Each simulation is repeated $H = 10{,}000$ times by permuting the initial torus. On the abscesses, the Schelling's threshold x ranging in $[0, 1]$. Lines indicate, respectively, the second (lower ticked line), the third (bold line), and the fourth (upper ticked line) quintile of the distribution of values obtained. Upper left panel indicates the number of iterations required for the model to converge. Upper middle and right panels report, respectively, the Moran's I and the FSI value obtained after model convergence. Bottom left panel shows the number of people who moved at least once in a simulation. Bottom middle and right panels display, respectively, the average and the total social welfare of the agents at the end of the iteration process. Social welfare is obtained from i-th agent's utility function (Equation 11). The color of the area indicates the two components of agents' utility after convergence is achieved: $\beta\alpha U_i^{color}(\bar{v};x)$ (lighter-colored area) and $\beta\alpha U_i^{friend}(\bar{v})$ (darker-colored area)

number of friendships becomes too high, there is an increasing disutility in locating close to few friends: for example, when degree centrality is 73, even if i is surrounded by all friends of her color, she is still far from 65 friends. This implies that as the degree increases, the location of friends becomes somewhat indifferent to agents, because for each friend found in one place, there will be many others left far apart, and most of the utility is obtained by the composition of the neighborhood: this is for example the case of agent 44, who despite the increase in her degree centrality, she remained consistently in her starting locations, next to 3 blue nodes, in all panels of Figure 13.

Moreover, it is worth stressing that because $\alpha = 0.5$, competing characteristics counteract each other, even if one of them is producing a disutility (e.g., social connections). Put differently, agents are able to cope with the disutility derived from one of their characteristics and maintain social welfare constant by letting Schelling's heuristic prevail over other utility's components in their relocation choices.
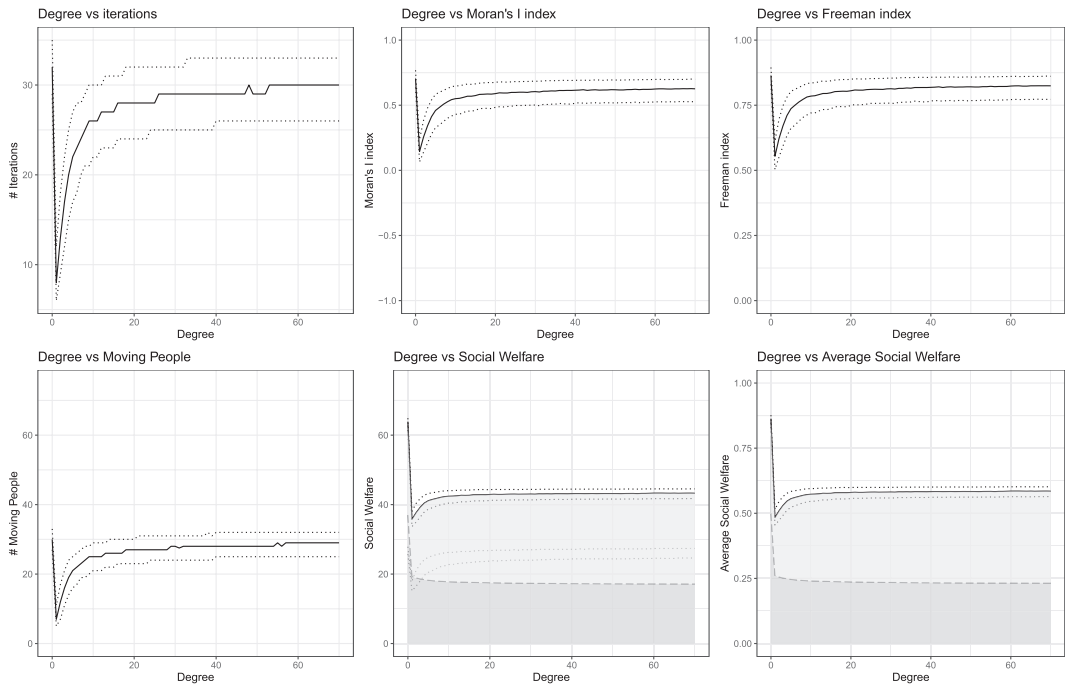
FIGURE 12 No moving costs ($\beta = 1$)—Fair utility from friendship and Schelling's heuristics ($\alpha = 0.5$)—Maximum value of the Schelling's threshold $x = 1$. Each simulation is repeated $H = 10,000$ times by permuting the initial torus and network connections. On the abscesses, the degree centrality (number of friends) k, ranging from 0 to 73. Lines indicate, respectively, the second (lower ticked line), the third (bold line), and the fourth (upper ticked line) quintile of the distribution of values obtained. Upper left panel indicates the number of iterations required for the model to converge. Upper middle and right panels report, respectively, the Moran's I and the FSI value obtained after model convergence. Bottom left panel shows the number of people who moved at least once in a simulation. Bottom middle and right panels display, respectively, the average and the total social welfare of the agents at the end of the iteration process. Social welfare is obtained from agents' utility function (Equation 11). The color of the area indicates the two components of agents' utility after convergence is achieved: $\beta \alpha U_i^{color}(\bar{v};x)$ (lighter-colored area) and $\beta \alpha U_i^{friend}(\bar{v})$ (darker-colored area)

5.5 | Robustness checks

We now test the robustness of our results when: (i) considering agents heterogeneous moving cost, and (ii) choosing a different method to generate the initial position of agents in the torus.

Exercise (i) allow us to mimic the situation when moving to certain areas is more expensive than moving to other areas, and thus consider the relationship between the price of moving to a house (included in the cost of movement) and the buyer's ability to pay for it. Specifically, we consider the following setting. Moving costs are very small for 70% of the cells in the torus (i.e., $\bar{c} = 0.001$ (i.e., these are the areas of the torus where the cost of the houses are relatively cheap), as in Figure 7), and they are very high for the remaining 30% of the cells (i.e., $\bar{c} = 0.99$, as in 8) (i.e., these are the areas of the torus where the cost of the houses are relatively expensive). The cells associated to higher costs are organized in two areas (neighborhoods). Both neighborhoods are formed by the same number of cells (i.e., 15 cells). Observe that moving costs are assumed to be fixed (i.e., $\gamma = 1$). We then compare the results obtained using this setting to those presented in Figure 7 of the paper, where we consider small moving costs (i.e., $\bar{c} = 0.001$). Complementing the
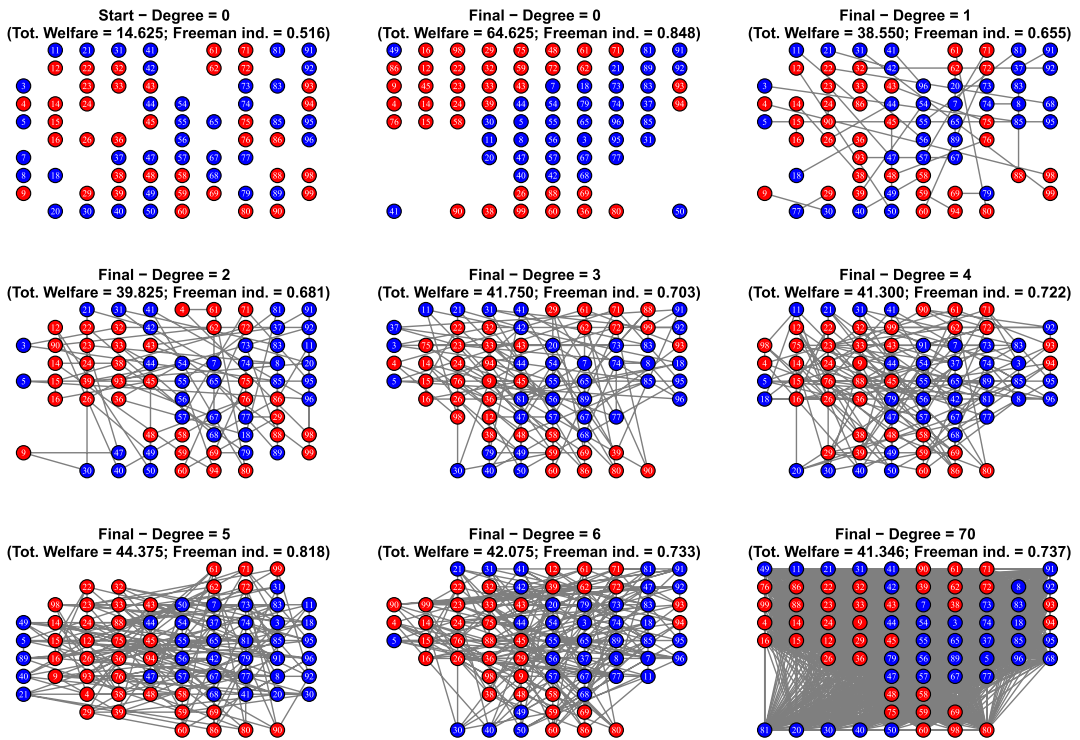
FIGURE 13 The Figure on the upper-left panel shows the starting position of the torus, and it indicates the values of total welfare and Freeman index when degree is equal to 0. Other figures show the final position of the torus corresponding to different levels of degree. Also for this case, we report the values of total welfare and Freeman index [Colour figure can be viewed at wileyonlinelibrary.com]

analysis presented in Sections 5.2 and 5.3, the scenarios investigated are those when agents' utility does not depend on friendship ($\alpha = 1$), Figure C1, it assigns equal weights to neighborhood composition and friends' distance ($\alpha = 0.5$), with $k = 3$, Figure C2, or when increasing agents' responsiveness to moving costs (β ranging in $[0, 1]$), Figure C3. In the figures, light and dark gray lines indicate, respectively, the outcome of simulations of the baseline results (those from Figure 7), and the outcome of simulations when considering heterogeneous moving costs. We find that the introduction of heterogeneous moving costs decreases significantly the number of moving agents, since now they have an additional constraint in the choice of a new location. As a consequence, we register that simulations take a shorter time to converge, that is, model iterations reduces, and agents' movements converge to a lower segregation status at the end of the process, that is both Moran and Freeman index reduce by approximately 30%. Consistently, also social welfare (both total and average) decreases. Results are qualitatively unchanged when considering variable costs (i.e., $\gamma = 1$), and they are, respectively, presented in Figure C4, C5, and C6.[12]

Results from exercise (ii) are presented in 10. These are obtained by generating a torus describing highly segregated or highly integrated situations. Using this method, we simulated 1000 instances of the torus featuring a Moran's I within a specific bound. Specifically, we generate instances of the torus with an initial value of Moran's I comprised between: (i) -0.50 and -0.40;

---

[12]Observe that results are qualitatively unchanged when considering a single neighborhood composed by 30% of the cells in the torus. Results are available upon request.

(ii) −0.40 and −0.30; (iii) −0.30 and −0.20; (iv) −0.20 and −0.10; (v) −0.10 and 0.00; (vi) 0.00 and 0.10; (vii) 0.10 and 0.20; (viii) 0.20 and 0.30; (ix) 0.30 and 0.40; and (x) 0.40 and 0.50. In doing so, we obtained 10,000 instances of the torus.[13] A number of interesting facts emerge.

First consider the case when moving costs and friendship are not included in the agents' utility function (i.e., $\alpha = 0$ and $\beta = 1$). Results from this setting are presented in Figure D1, where darker lines indicate the results obtained when considering a more and more initial integrated status. When there is a low incentive to move close to agents with the same color type (i.e., Schelling's threshold is set lower than 0.5), the initial situation of the torus is almost unchanged at the end of simulations. Of course, this implies that differences in the segregation status among the instances of the torus will be preserved at the end of the simulations. Interestingly, however, when we increase the propensity for locating in a neighborhood with same-color agents, final segregation increases very rapidly when considering an initial integrated situation, and very slowly when starting from an initial segregated situation. As a result, the final segregation status of all the instances of the torus, rapidly converge to similar values. It follows that, at least when Schelling's heuristics is significantly at play, the choice of the initial status mainly affects the number of iterations and moving agents in this context (i.e., these values will be higher for an initial integrated status, and lower for an initial segregated status), but our main results are substantially unchanged.

Now consider when fair moving costs are introduced in the utility function (i.e., $\bar{c} = 0.5$), there is no contribution of friendship to utility ($\alpha = 1$), Schelling's threshold is set at its maximal value ($x = 1$), and we progressively increase the responsiveness of agents to moving cost (β ranging in [0, 1]). Results from this exercise are presented in Figures D2, and D3, and represent the scenario when moving costs are fixed or variable, respectively. When responsiveness to moving costs is high (i.e., $0.8 \leq \beta \leq 1$), differences in the initial status of the instances of the torus are preserved after simulations. However, in all other cases (i.e., $\beta \leq 0.8$), again we observe that all simulations rapidly converge to a similar segregation status regardless of the initial torus considered. This implies that when moving costs are considered, only when the responsiveness to them is very high then the choice of the initial torus matters in determining the final segregation status. Since this situation is hard to observe, we focus on the scenario where there is a fair responsiveness to moving costs ($\beta = 0.5$), and we test the robustness of our results to the choice of the initial status of the torus when increasing Schelling's threshold value (x). This is presented in Figures D4 and D5, respectively, for fixed and moving costs. Consistent with our previous finding, we observe that simulations return significantly different results only when Schelling's heuristics plays a small role in the determination of agents' utility. Instead, when x becomes larger, the choice of the initial status mostly determine a different number of iterations and moving agents, but the final status of segregation and the value of welfare rapidly converge to similar values. Of course, whereas in the case of no moving costs the final outcome of simulations is very similar, in this situation still some differences are observed. The reason is that friction to movements are now at play.

Finally, consider the inclusion of friendship in agents' utility function. In our first experiment, we investigate how our results are affected by the choice of the initial torus when increasing Schelling's threshold value considering the scenario where we introduce a fair utility from friendship ($\alpha = 0.5$), and disregard moving costs ($\beta = 1$), assuming that $k = 3$, Figure D6, and where a

---

[13]The minimum and maxim values of the Moran I that we were able to obtain in this case is −0.4807 and 0.4980, respectively. Observe that it is impossible to create a torus mimicking a situation of perfect integration or perfect segregation (i.e., a torus with Moran's I approximating the value 1), because not all positions are occupied by an agent.

fair responsiveness to fixed or variable moving costs is considered (i.e., $\beta = 0.5$ and $\bar{c} = 0.5$), respectively, Figures D7 and D8. Since now agents have less interest in being located close to those sharing their color type, because they are equally attracted by the position of their friends, they tend to reduce their movements and maintain the status quo in the torus. Consequently, this is the only case when differences in the segregation status observed at the beginning of simulations are always preserved at the end of the simulations: that is, depending on their initial status, agents will end up in a situation of smaller or higher segregation. Also in this case, however, we do not find that the initial position of the torus affects the behavior of agents. When increasing the parameter of the model controlling for the preference of agents for being located close to agents of the same color type, agents will all behave in the exact same way, that is they will end up in a situation characterized by a higher segregation, and such increase in the segregation of the torus will be the same regardless of the initial torus chosen. In other words, since friendship reduces the incentive to movements, the initial status of the torus has the only effect to shift the magnitude of segregation metrics registered.

In our second experiment, we test how our results are affected by the choice of the initial torus when increasing the degree centrality of agents (k). Similar to the situation when we increase friction to movements determined by moving costs, we observe that the choice of the initial status mostly determine a different number of iterations and moving agents, but the final status of segregation and the value of welfare rapidly converge to similar values when increasing the number of friends.

The takeaways from this exercise are three then. First, regardless of the level of segregation, agents always move in our setting, even when the simulation begin with a situation of high segregation. Second, the initial position of agents does not significantly affect the final segregation status of simulations with or without considering moving costs (unless the responsiveness to these is extremely high). Third, moving costs and friendship are relevant elements of friction against Schelling's heuristic, which can prevent radical changes in the torus. However, they do not affect the reaction of agents to an exogenous increase of their preference toward segregation.

6 | DISCUSSION AND CONCLUSIONS

This paper presented an extension of the original racial and residential segregation model by Schelling. Specifically, the aim was to investigate whether and how model's predictions can be improved in order to incorporate solutions of limited segregation equilibria.

The evidence provided by our simulations suggests that a possible explanation for the formation of racially mixed areas might be the presence of moving costs and the effect of social linkages. Moving costs, regardless of whether they are fixed or variable, consistently determines phenomena of local inertia, preventing agents to leave their neighborhood for another that better suits with their set of preferences. Interestingly, a similar outcome is observed when agents have a stronger preference for social linkages over Schelling's heuristic. In this case, agents' movements are constrained by the tension exerted by friends' position, who are in turn constrained in their movements by their friends. Perhaps unexpectedly, local inertia is found also to be associated with lower levels of social welfare.

Another interesting insight provided by our study is that, whenever homophily effects are constrained by the existence of competing characteristics with which agents equally identify (e.g., ethnicity and social connections), certain characteristics tend to prevail in the formation

relocation choices. The reason is straightforward. It is easier for agents to identify a neighborhood where only one characteristic is predominant. Future research should be dedicated to understand what are these characteristics that tend to define one's own identity and drive relocation choice.

This investigation has also highlighted that whenever homophily requires to combine multiple characteristics, the generic agent finds it difficult to find a neighborhood that will improve her levels of welfare: for example, a racially mixed neighborhood where the majority is composed by people of her own color, and the minority is represented by her social connections. This suggests that suboptimal levels of welfare might be endemic in context where multiple elements concur to the definition of one's own identity.

The very general setup of the model allows many interesting extensions that we leave for future research.

In the present model, we kept Schelling's heuristic and the structure of the friendship network separated. This was done on purpose in order not to mix the effects of the two, but this modeling choice implies that the process shaping the racial distribution of friends is purely random and is not determined by a preference for homophily. Evidence is at odd. As recalled by Jackson (2019, p. 109), simple accounting tells us that individuals in the minority group will end up having more friends from the majority group on average than individuals from the majority have with ones in the minority group. Considering homophily this effect would be magnified, rationalizing the striking evidence reported by Jackson: "Guess how many black friends the typical white person in the U.S. has—where a friend is someone with whom that person 'regularly discussed important matters'? Zero." If friendship formation is lead by homophily, the two processes shaping Schelling's heuristic and friendship formation interact. A condition worth exploring in future research.

A second aspect that could add new insights to the model would be the possibility of forming or dissolving friendship at every movement on the chequerboard. Moving implies costs but also offers opportunity to create new friends and confirm the old ones. When social linkages varies with location changes, the new friends in the neighborhood reinforce the propensity not to further move. On the contrary, if past social linkages remain relevant, the incentive to go back to the previous location persists. This change in the model's setup would allow to study the role of past and present social linkages of migrants and the ultimate effect on segregation and welfare in the new location and in previous one.

Finally, the evidence of power laws, fat tails, Pareto, and scale-free degree distributions is typical of social networks (Goyal, 2009; Newman, 2005). The model's assumption of a uniform distribution of friends is purely exemplificative and can be modified at no particular cost. In this case, centrality and degree heterogeneity would start to influence the segregation equilibria, since the network externality is associated to node centrality and the movement of central nodes brings a greater influence on the decision of poorly connected nodes. Similar extension can be applied to a social linkages that are directed and or weighted.

REFERENCES

Akerlof, G. A., & Kranton, R. E. (2000). Economics and identity. *The Quarterly Journal of Economics*, *115*(3), 715–753.

Akerlof, G. A., & Kranton, R. E. (2012). *Identity economics: How our identities shape our work, wages, and well-being*. Princeton University Press.

Anselin, L. (1995). Local indicators of spatial association. LISA. *Geographical analysis*, *27*(2), 93–115.

Atkinson, A. B., et al. (1970). On the measurement of inequality. *Journal of Economic Theory*, *2*(3), 244–263.

Axelrod, R. (2013). Advancing the art of simulation in the social sciences. *Simulating social phenomena* (chapter 1, 21–40). Springer.

Baerveldt, C., Duijn, M. A., Vermeij, L., & Hemert, D. A. (2004). Ethnic boundaries and personal choice. Assessing the influence of individual inclinations to choose intra-ethnic relationships on pupils' networks. *Social Networks*, *26*(1), 55–74.

Barabási, A. L. (2016). *Network science*. Cambridge University Press.

Batty, M. (2013). *The new science of cities*. MIT Press.

Bernard, S., & Willer, R. (2007). A wealth and status-based model of residential segregation. *The Journal of Mathematical Sociology*, *31*(2), 149–174.

Benenson, I., Hatna, E., & Or, E. (2009). From schelling to spatially explicit modeling of urban ethnic and economic residential dynamics. *Sociological Methods & Research*, *37*(4), 463–497.

Benito-Ostolaza, J. M., Brañas-Garza, P., Hernández, P., & Sanchis-Llopis, J. A. (2015). Strategic behaviour in Schelling dynamics: Theory and experimental evidence. *Journal of Behavioral and Experimental Economics*, *57*, 134–147.

Bojanowski, M., & Corten, R. (2014). Measuring segregation in social networks. *Social Networks*, *39*, 14–32.

Bona, J. L., & Santos, M. S. (1997). On the role of computation in economic theory. *Journal of Economic Theory*, *72*(2), 241–281.

Calvo-Armengol, A., & Jackson, M. O. (2004). The effects of social networks on employment and inequality. *American Economic Review*, *94*(3), 426–454.

Calvo-Armengol, A., & Jackson, M. O. (2007). Networks in labor markets: Wage and employment dynamics and inequality. *Journal of Economic Theory*, *132*(1), 27–46.

Clark, W. A. (1991). Residential preferences and neighborhood racial segregation: A test of the Schelling segregation model. *Demography*, *28*(1), 1–19.

de Marti, J., & Zenou, Y. (2017). Segregation in friendship networks. *Journal of Behavioral and Experimental, Economics*, *119*(3), 656–708.

Easley, D., & Kleinberg, J. (2010). *Networks, crowds, and markets*. Cambridge University Press.

Easterly, W. (2009). Empirics of strategic interdependence: The case of the racial tipping point. *The BE Journal of Macroeconomics*, *9*, 1.

Fagiolo, G., Valente, M., & Vriend, N. J. (2007). Segregation in networks. *Journal of Economic Behavior & organization*, *64*(3–4), 316–336.

Fossett, M. (2011). Generative models of segregation: Investigating model-generated patterns of residential segregation by ethnicity and socioeconomic status. *Journal of Mathematical Sociology*, *35*(1–3), 114–145.

Freeman, L. C. (1978). Segregation in social networks. *Sociological Methods & Research*, *6*(4), 411–429.

Geary, R. C. (1954). The contiguity ratio and statistical mapping. *The Incorporated Statistician*, *5*(3), 115–146.

Glaeser, E. L., & Vigdor, J. L. (2012). *The end of the segregated century: Racial separation in America's neighborhoods, 1890–2010* (Technical Report Civic Report No. 66). Manhattan Institute.

Goyal, S. (2009). *Connections: An introduction to the economics of networks*. Princeton University Press.

Hatna, E., & Benenson, I. (2012). The Schelling model of ethnic residential dynamics: Beyond the integrated-segregated dichotomy of patterns. *Journal of Artificial Societies and Social Simulation*, *15*(1), 6.

Henderson, J. V. (2014). *Economic theory and the cities*. Academic Press.

Henry, A. D., Pralatb, P., & Zhang, C. Q. (2011). Emergence of segregation in evolving social networks. *Proceedings of the National Academy of Science*, *108*(21), 8605–8610.

Hensher, D. A., Rose, J. M., & Greene, W. H. (2005). *Applied choice analysis: A primer*. Cambridge University Press.

Ioannides, Y. M. (2013). *From neighborhoods to nations: The economics of social interactions*. Princeton University Press.

Jackson, M. O. (2007). *Social structure, segregation, and economic behavior*. Presented as the Nancy Schwartz Memorial Lecture.

Jackson, M. O. (2010). *Social and economic networks*. Princeton University Press.

Jackson, M. O. (2019). *The human network: How your social position determines your power, beliefs, and behaviors*. Pantheon.

Lee, C. (2004). Emergence and universal computation. *Metroeconomica*, *55*(2–3), 219–238.

Logan, J. R., & Stults, B. J. (2011). *The persistence of segregation in the metropolis: New findings from the 2010 census* (Technical report, US2010 Project Report).

Massey, D. S., & Denton, N. A. (1988). The dimensions of residential segregation. *Social Forces*, *67*(2), 281–315.

McPherson, M., Smith-Lovin, L., & Cook, J. M. (2001). Birds of a feather: Homophily in social networks. *Annual Review of Sociology*, *27*(1), 415–444.

Mele, A. (2017). A structural model of dense network formation. *Econometrica*, *85*(3), 825–850.

Möbius, M. M., & Rosenblat, T. S. (2001). *The process of ghetto formation evidence from Chicago*.

Moran, P. A. (1950). A test for the serial independence of residuals. *Biometrika*, *37*(1/2), 178–181.

Newman, M. (2010). *Networks: An introduction*. OUP.

Newman, M. E. (2005). Power laws, Pareto distributions and Zipf's law. *Contemporary Physics*, *46*(5), 323–351.

Ong, C. B. (2017). Tipping points in Dutch big city neighborhoods. *Urban Studies*, *54*(4), 1016–1037.

Pancs, R., & Vriend, N. J. (2007). Schelling's spatial proximity model of segregation revisited. *Journal of Public Economics*, *91*(7), 1–24.

Rosser, J. J. B. (2011). Post Keynesian perspectives and complex ecologic economic dynamics. *Metroeconomica*, *62*(1), 96–121.

Schelling, T. C. (1969). Models of segregation. *The American Economic Review*, *59*(2), 488–493.

Schelling, T. C. (1971a). Dynamic models of segregation. *Journal of Mathematical Sociology*, *1*(2), 143–186.

Schelling, T. C. (1971b). On the ecology of micromotives. *The Public Interest*, *25*, 59.

Schelling, T. C. (2006). *Micromotives and macrobehavior*. WW Norton & Company.

Sethi, R., & Somanathan, R. (2004). Inequality and segregation. *Journal of Political Economy*, *112*(6), 1296–1321.

Silver, D., Byrne, U., & Patrick, A. (2021). Venues and segregation: A revised Schelling model. *PLoS one*, *16*(1), e0242611.

Stadtfeld, C. K. T., & Vörös, A. (2020). The emergence and stability of groups in social networks. *Social Networks*, *60*, 129–145.

Taylor, H. (1984). The use of maps in the study of the black ghetto-formation process: Cincinnati, 1802–1910. *Historical Methods: A Journal of Quantitative and Interdisciplinary History*, *17*(2), 44–58.

van Ham, M., Tammaru, T., de Vuijst, E., & Zwiers, M. (2016). *Spatial segregation and socio-economic mobility in European cities*. Institute for the Study of Labor (IZA).

Velupillai, K. V., & Zambelli, S. (2015). Simulation, computation and dynamics in economics. *Journal of Economic Methodology*, *22*(1), 1–27.

Vermeij, L., Duijn, M. A. J., & Baerveldt, C. (2009). Ethnic segregation in context: Social discrimination among native Dutch pupils and their ethnic minority classmates. *Social Networks*, *31*(4), 230–239.

Vinković, D., & Kirman, A. (2006). A physical analogue of the Schelling model. *Proceedings of the National Academy of Sciences*, *103*(51), 19261–19265.

Young, H. P. (2001). *Individual strategy and social structure: An evolutionary theory of institutions*. Princeton University Press.

Zhang, J. (2004). A dynamic model of residential segregation. *Journal of Mathematical Sociology*, *28*(3), 147–170.

Zhang, J. (2011). Tipping and residential segregation: A unified Schelling model. *Journal of Regional Science*, *51*(1), 167–193.

APPENDIX A

FIGURES: LOW MOVING COSTS

This appendix extends the results presented in Section (5) by using lower levels of moving costs ($\overline{c} = 0.01$) with respect to the main analysis ($\overline{c} = 0.5$). Footnote 10 details the rest of the parameter set.

In Figures A1 and A2, we progressively increase the responsiveness of i's utility to a change in moving costs (β), when these are, respectively, fixed and variable. The results show that model outcome remains qualitatively unchanged with respect to the main analysis (see for comparison Section 5.2, and Figures 5 and 6): (i) there is a monotonic relation between agents' level of responsiveness and the number of individual movements; (ii) model outcome tends to mimic Schelling's result when the role of moving cost becomes least significant (i.e., high values of β); (iii) there is a negative relation between moving costs and social welfare; (iv) when agents are least subject to the constraints of moving costs, because β exceeds a certain threshold value, simulations always reproduce the same segregation dynamics in terms of both number of iterations and moving people, and of segregation and welfare indexes: that is, the final configuration of the grid is unaffected by any further increase of β. Only a significant change occurs in our findings, and that is when considering the case of fixed costs. Here we register a dramatic downshift in
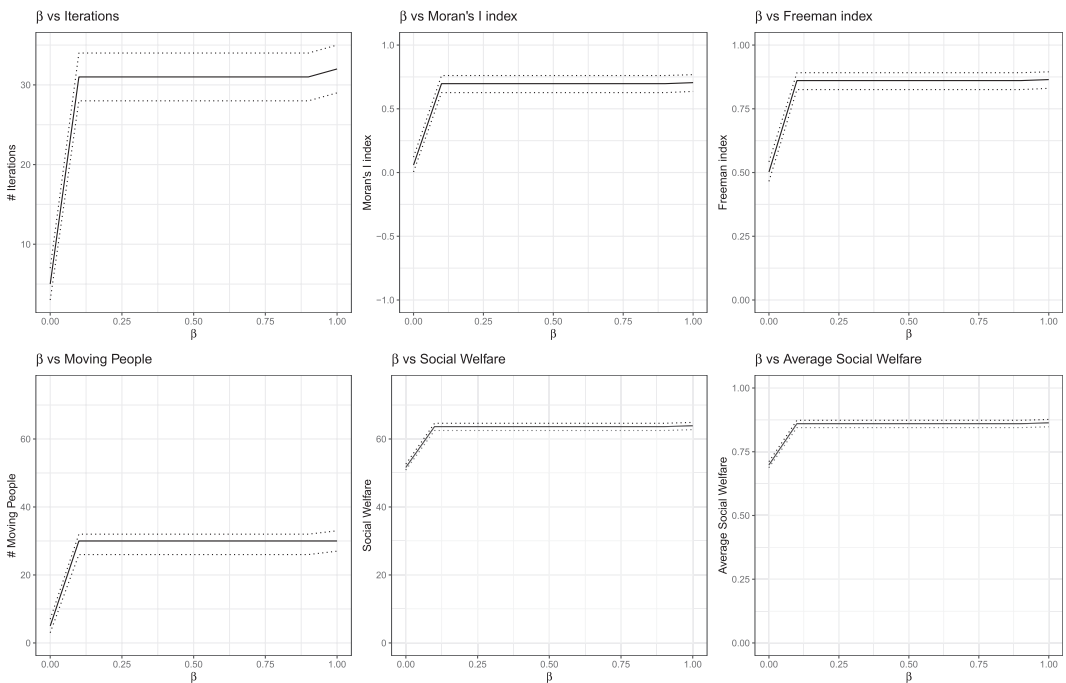
FIGURE A1 Low fixed moving costs ($\gamma = 1$, $\overline{c} = 0.01$)—Maximum value of the Schelling's threshold $x = 1$ —No contribution of friendship to utility ($\alpha = 1$). Each simulation is repeated $H = 100$ times by permuting the initial torus. On the abscesses, we have parameter β ranging in [0, 1]. Lines indicate, respectively, the second (lower ticked line), the third (bold line), and the fourth (upper ticked line) quintile of the distribution of values obtained. Upper left panel indicates the number of iterations required for the model to converge. Upper middle and right panels report, respectively, the Moran's I and the FSI value obtained after model convergence. Bottom left panel shows the number of people who moved at least once in a simulation. Bottom middle and right panels display, respectively, the average and the total social welfare of the agents at the end of the iteration process. Social welfare is obtained from the component $\beta\alpha U_i^{color}(\overline{v};x)$ of ith agent utility function (Equation 11)
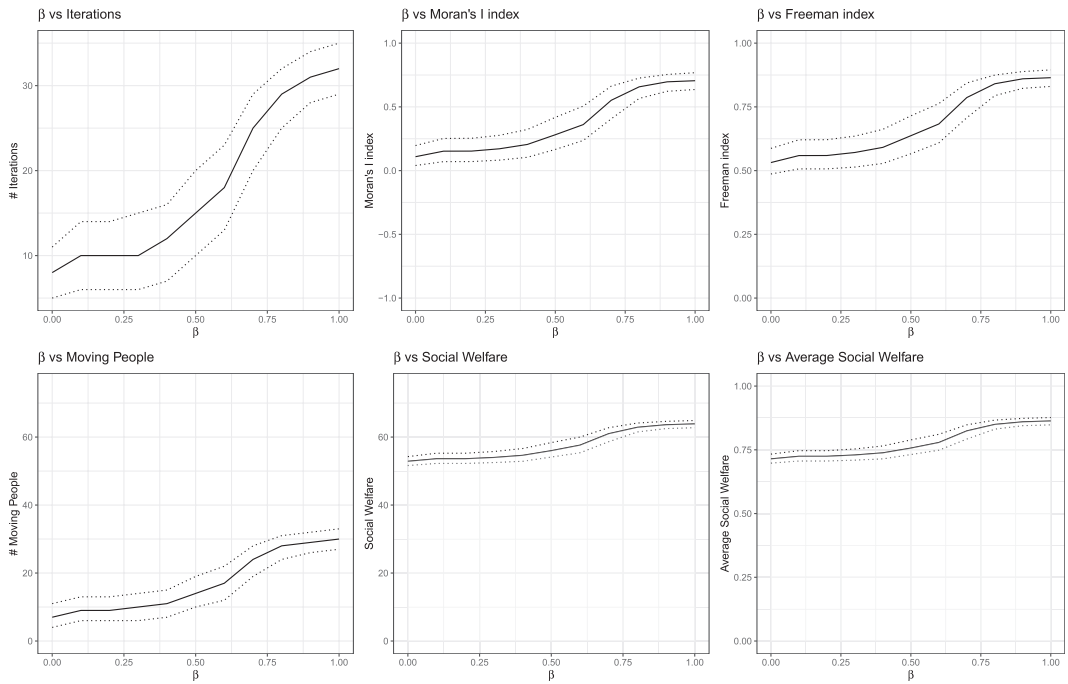
FIGURE A2 Low variable moving costs ($\gamma = 0$, $\bar{c} = 0.01$)—Maximum value of the Schelling's threshold $x = 1$—No contribution of friendship to utility ($\alpha = 1$). Each simulation is repeated $H = 10,000$ times by permuting the initial torus. On the abscesses, we have parameter β ranging in [0, 1]. Lines indicate, respectively, the second (lower ticked line), the third (bold line), and the fourth (upper ticked line) quintile of the distribution of values obtained. Upper left panel indicates the number of iterations required for the model to converge. Upper middle and right panels report, respectively, the Moran's I and the FSI value obtained after model convergence. Bottom left panel shows the number of people who moved at least once in a simulation. Bottom middle and right panels display, respectively, the average and the total social welfare of the agents at the end of the iteration process. Social welfare is obtained from the component $\beta \alpha U_i^{color}(\bar{v};x)$ of ith agent utility function (Equation 11)

the threshold value of β over which considered metrics become constant: that is, from $\beta > 0.75$ in the main analysis to $\beta > 0.10$. The reason is that moving costs are fixed and close to zero, hence they have substantially no impact on the relocation choices of the agent: that is, agents are free to choose every empty cell regardless of its distance, because their utility level remains substantially unaltered by moving costs. The same is not true when considering variable moving costs. This is because costs increases with distance, and thus they still represents a constraint for agents. As a result, the model outcome when considering low variable moving costs mimics the case considered in the main analysis, and no meaningful changes are observed.

In Figures A3 and A5, we progressively increase the responsiveness of i to neighborhood composition (x), when moving costs are, respectively, fixed and variable. This complements the analysis presented in Figures 8 and 10 in Section 5.3. Results remain unaffected with respect to the main analysis. The responsiveness of the model outcome to a change in x is the same in the two set of exercises. When agents do not care for the level of homophily in the composition of their neighborhood ($x < 0.5$), there is no incentive to move and convergence is achieved in one iteration as a result of the presence of moving costs. The same logic applies when we replicate the previous exercise and we increase the degree centrality from $k = 0$ to $k = 3$, comparing Figures A4 and A6 with, respectively, Figures 9 and 11. All in all, segregation dynamics observed in this context remains unaltered when decreasing the level of moving costs.
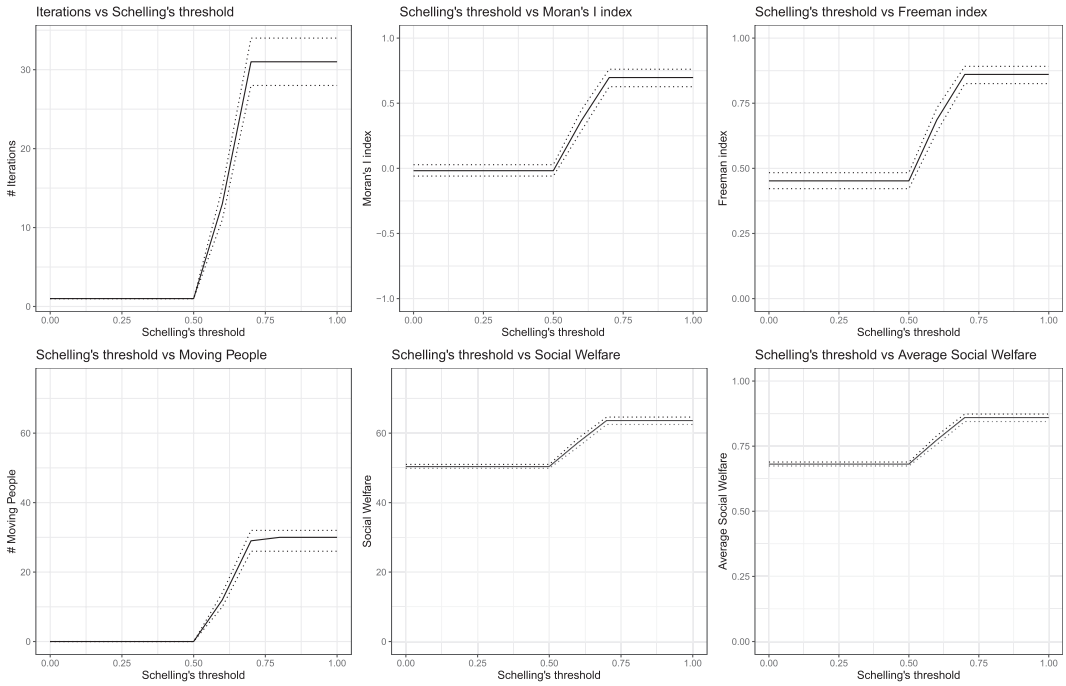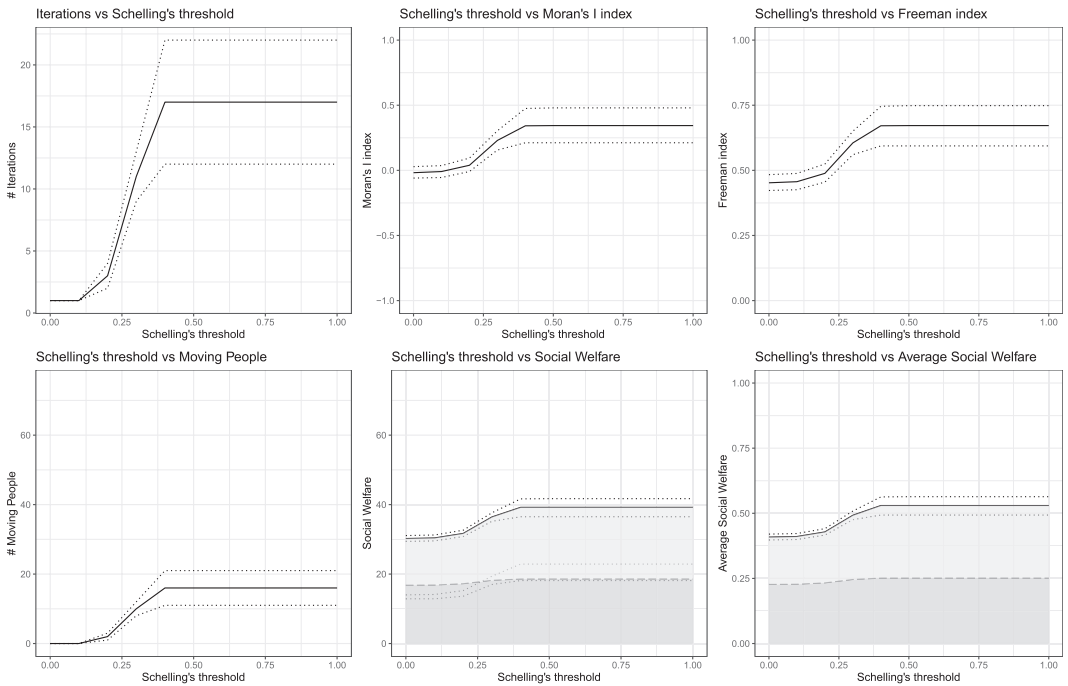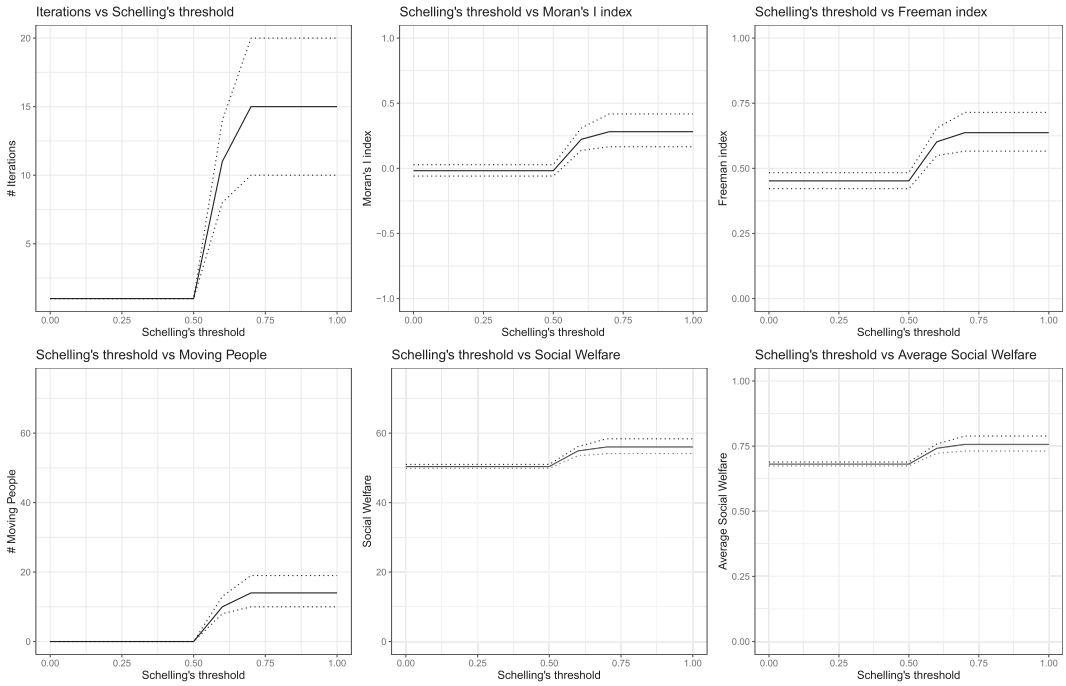
FIGURE A3 Low fixed moving costs ($\beta = 0.5$, $\gamma = 1$, $\bar{c} = 0.01$)—No contribution of friendship to utility ($\alpha = 1$). Each simulation is repeated $H = 10,000$ times by permuting the initial torus. On the abscesses, we have Schelling's threshold x ranging in [0, 1]. Lines indicate, respectively, the second (lower ticked line), the third (bold line), and the fourth (upper ticked line) quintile of the distribution of values obtained. Upper left panel indicates the number of iterations required for the model to converge. Upper middle and right panels report, respectively, the Moran's I and the FSI value obtained after model convergence. Bottom left panel shows the number of people who moved at least once in a simulation. Bottom middle and right panels display, respectively, the average and the total social welfare of the agents at the end of the iteration process. Social welfare is obtained from the component $\beta\alpha U_i^{color}(\bar{v};x)$ of ith agent utility function (Equation 11)
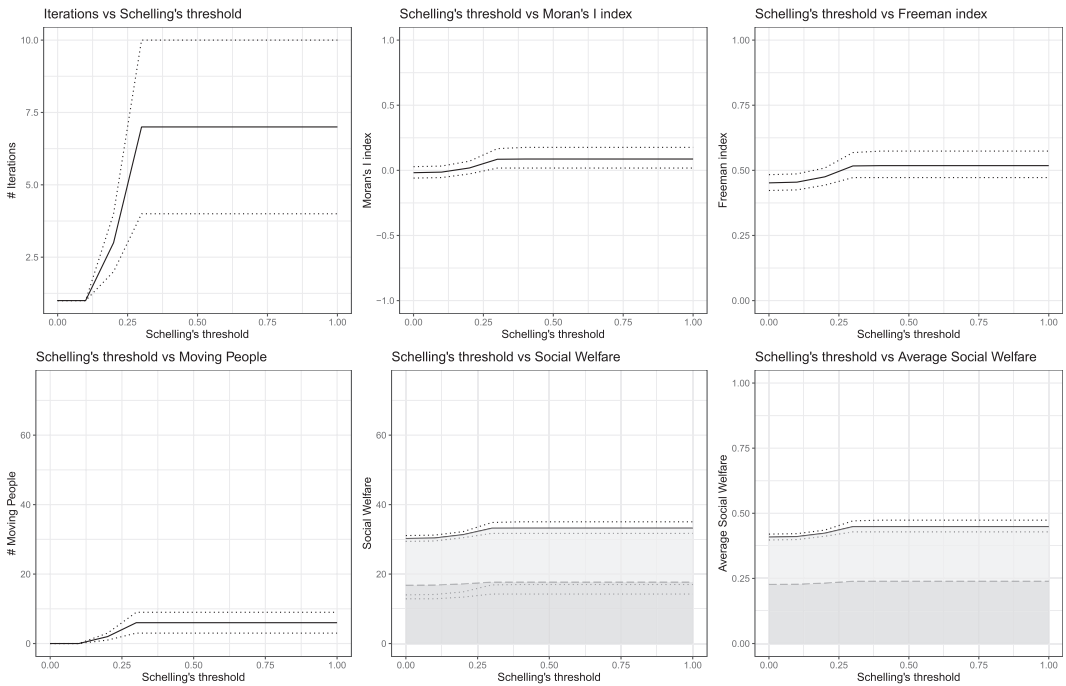
FIGURE A4 Low fixed moving costs ($\beta = 0.5$, $\gamma = 1$, $\bar{c} = 0.01$)—Fair contribution of friendship to utility and 3 friends ($\alpha = 0.5, k = 3$). Each simulation is repeated $H = 10,000$ times by permuting the initial torus. On the abscesses, we have Schelling's threshold x ranging in $[0, 1]$. Lines indicate, respectively, the second (lower ticked line), the third (bold line), and the fourth (upper ticked line) quintile of the distribution of values obtained. Upper left panel indicates the number of iterations required for the model to converge. Upper middle and right panels report, respectively, the Moran's I and the FSI value obtained after model convergence. Bottom left panel shows the number of people who moved at least once in a simulation. Bottom middle and right panels display, respectively, the average and the total social welfare of the agents at the end of the iteration process. Social welfare is obtained from the component $\beta\alpha U_i^{color}(\bar{v};x)$ of ith agent utility function (Equation 11). The color of the area indicates the two components of agents' utility after convergence is achieved: $\beta\alpha U_i^{color}(\bar{v};x)$ (lighter-colored area) and $\beta\alpha U_i^{friend}(\bar{v})$ (darker-colored area)

FIGURE A5 Low variable moving costs ($\beta = 0.5$, $\gamma = 0$, $\bar{c} = 0.01$)—No contribution of friendship to utility ($\alpha = 1$). Each simulation is repeated $H = 10{,}000$ times by permuting the initial torus. On the abscesses, we have Schelling's threshold x ranging in [0, 1]. Lines indicate, respectively, the second (lower ticked line), the third (bold line), and the fourth (upper ticked line) quintile of the distribution of values obtained. Upper left panel indicates the number of iterations required for the model to converge. Upper middle and right panels report, respectively, the Moran's I and the FSI value obtained after model convergence. Bottom left panel shows the number of people who moved at least once in a simulation. Bottom middle and right panels display, respectively, the average and the total social welfare of the agents at the end of the iteration process. Social welfare is obtained from the component $\beta\alpha U_i^{color}(\bar{v};x)$ of ith agent utility function (Equation 11)

FIGURE A6 Low variable moving costs ($\beta = 0.5$, $\gamma = 0$, $\bar{c} = 0.01$)—Fair contribution of friendship to utility and 3 friends ($\alpha = 0.5, k = 3$). Each simulation is repeated $H = 10{,}000$ times by permuting the initial torus. On the abscesses, we have Schelling's threshold x ranging in [0, 1]. Lines indicate, respectively, the second (lower ticked line), the third (bold line), and the fourth (upper ticked line) quintile of the distribution of values obtained. Upper left panel indicates the number of iterations required for the model to converge. Upper middle and right panels report, respectively, the Moran's I and the FSI value obtained after model convergence. Bottom left panel shows the number of people who moved at least once in a simulation. Bottom middle and right panels display, respectively, the average and the total social welfare of the agents at the end of the iteration process. Social welfare is obtained from the component $\beta\alpha U_i^{color}(\bar{v};x)$ of ith agent utility function (Equation 11). The color of the area indicates the two components of agents' utility after convergence is achieved: $\beta\alpha U_i^{color}(\bar{v};x)$ (lighter-colored area) and $\beta\alpha U_i^{friend}(\bar{v})$ (darker-colored area)

APPENDIX B

FIGURES: HIGH MOVING COSTS

This appendix extends the results presented in Section (5) by using higher levels of moving costs ($\bar{c} = 0.99$) with respect to the main analysis ($\bar{c} = 0.5$). Footnote 10 details the rest of the parameter set.

In Figures B1 and B2, we progressively increase the responsiveness of i's utility to a change in moving costs (β), when these are, respectively, fixed and variable. As in the case of 7, the results show that most model outcome remains qualitatively unchanged with respect to the main analysis when considering fixed moving costs (see for comparison Section 5.2 and Figure 5). There is only a significant difference with respect to the main analysis, and this is the level of responsiveness of the model outcome when β is low and agents are most subject to moving costs. In these cases, there are no incentives to move: that is, the process stops after one simulation and the initial configuration of the grid remains unaltered. When considering the case of variable moving
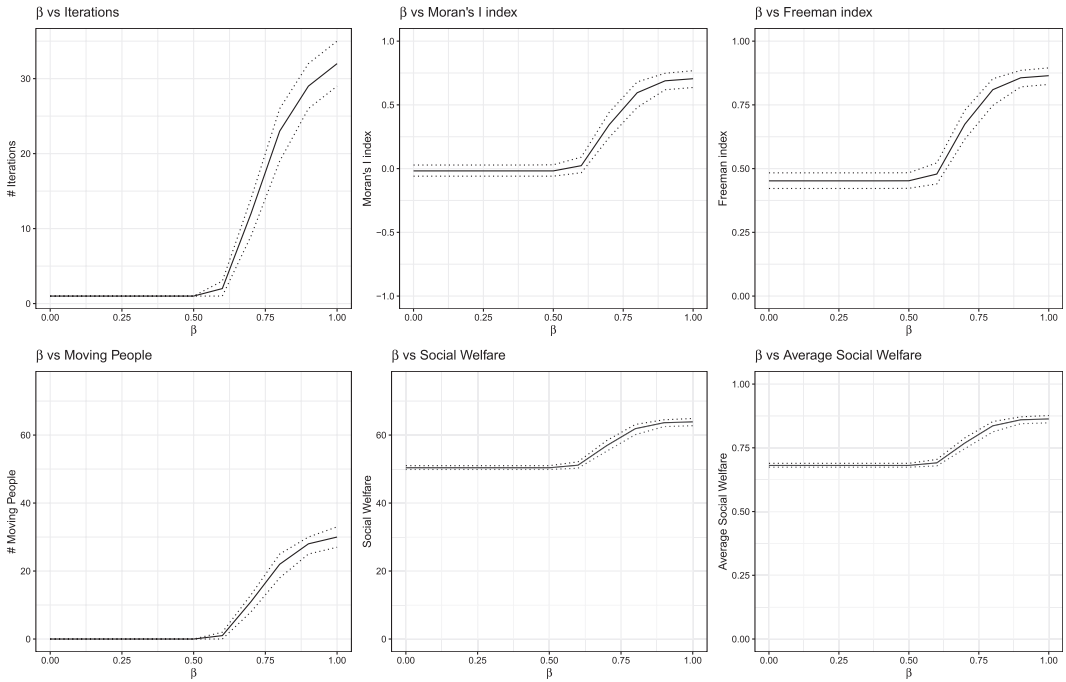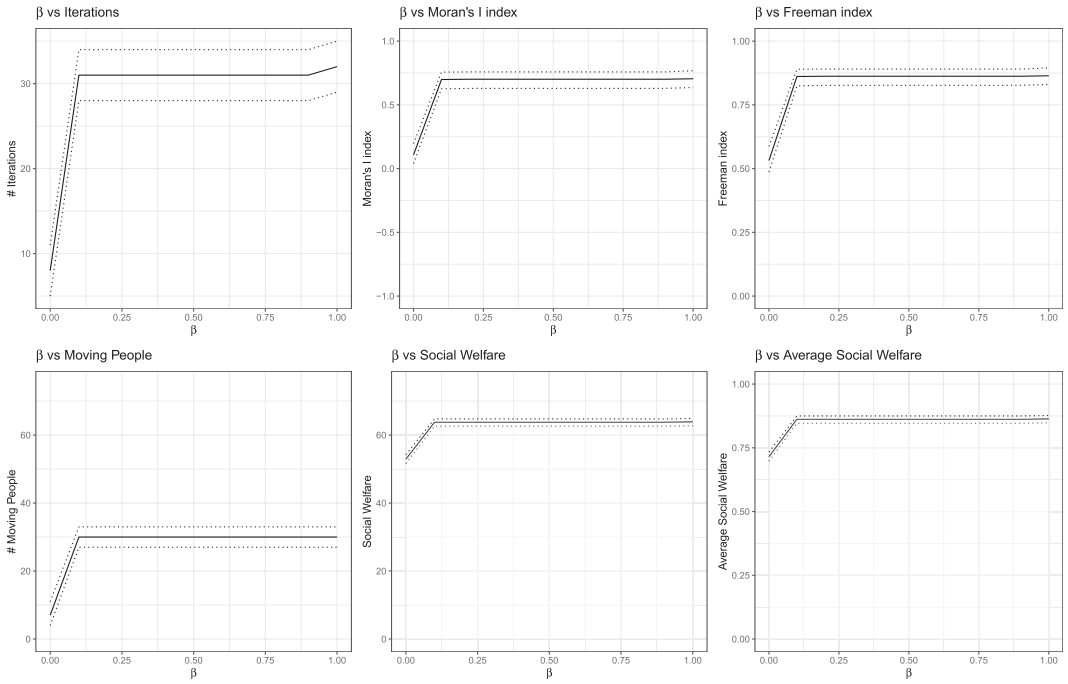
FIGURE B1 High fixed moving costs ($\gamma = 1$, $\bar{c} = 0.99$)—Maximum value of the Schelling's threshold $x = 1$ v—No contribution of friendship to utility ($\alpha = 1$). Each simulation is repeated $H = 10,000$ times by permuting the initial torus. On the abscesses, we have parameter β ranging in [0, 1]. Lines indicate, respectively, the second (lower ticked line), the third (bold line), and the fourth (upper ticked line) quintile of the distribution of values obtained. Upper left panel indicates the number of iterations required for the model to converge. Upper middle and right panels report, respectively, the Moran's I and the FSI value obtained after model convergence. Bottom left panel shows the number of people who moved at least once in a simulation. Bottom middle and right panels display, respectively, the average and the total social welfare of the agents at the end of the iteration process. Social welfare is obtained from the component $\beta\alpha U_i^{color}(\bar{v};x)$ of ith agent utility function (Equation 11)
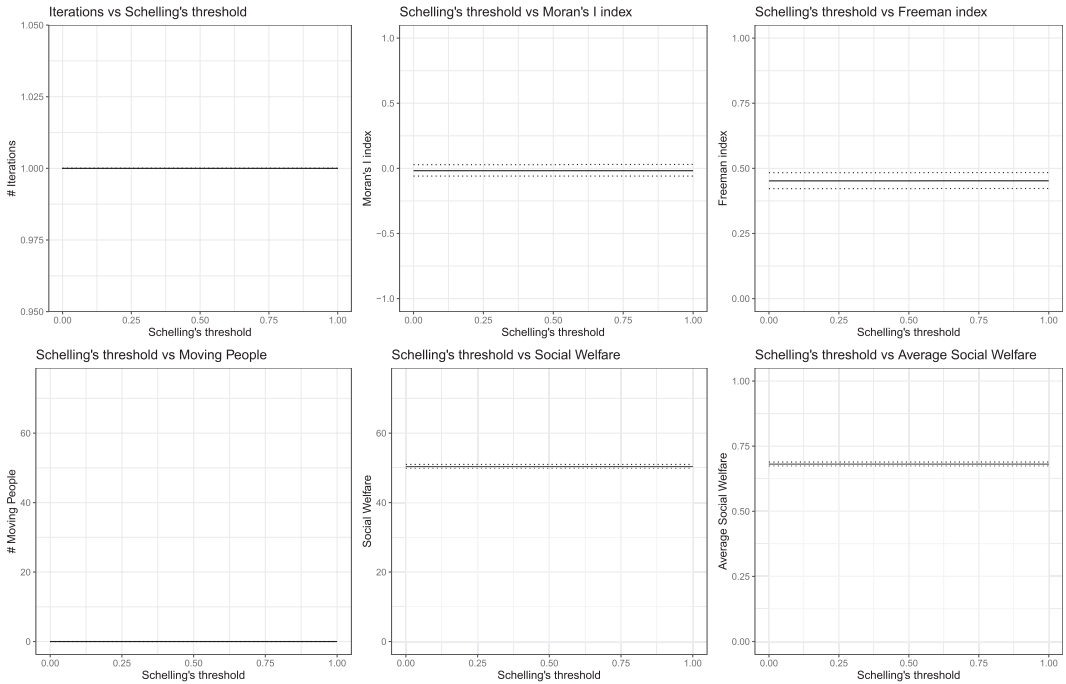
costs instead (see for comparison Section 5.2 and Figure 6), things change radically. The choice to relocate has such a negative impact on agents' utility in this context, that relocation constraints are substantially the same regardless of the value of β. Agents move in the same way, and the same segregation dynamics are observed whenever $\beta > 0$: that is, both number of iterations and moving people, and of segregation and welfare indexes remain constant regardless of the value of the parameter. A discussion about the rest of the figures is contained in Section 5.3.

FIGURE B2 High variable moving costs ($\gamma = 0$, $\bar{c} = 0.99$)—Maximum value of the Schelling's threshold $x = 1$—No contribution of friendship to utility ($\alpha = 1$). Each simulation is repeated $H = 10{,}000$ times by permuting the initial torus. On the abscesses, we have parameter β ranging in $[0, 1]$. Lines indicate, respectively, the second (lower ticked line), the third (bold line), and the fourth (upper ticked line) quintile of the distribution of values obtained. Upper left panel indicates the number of iterations required for the model to converge. Upper middle and right panels report, respectively, the Moran's I and the FSI value obtained after model convergence. Bottom left panel shows the number of people who moved at least once in a simulation. Bottom middle and right panels display, respectively, the average and the total social welfare of the agents at the end of the iteration process. Social welfare is obtained from the component $\beta\alpha U_i^{color}(\bar{v};x)$ of ith agent utility function (Equation 11)
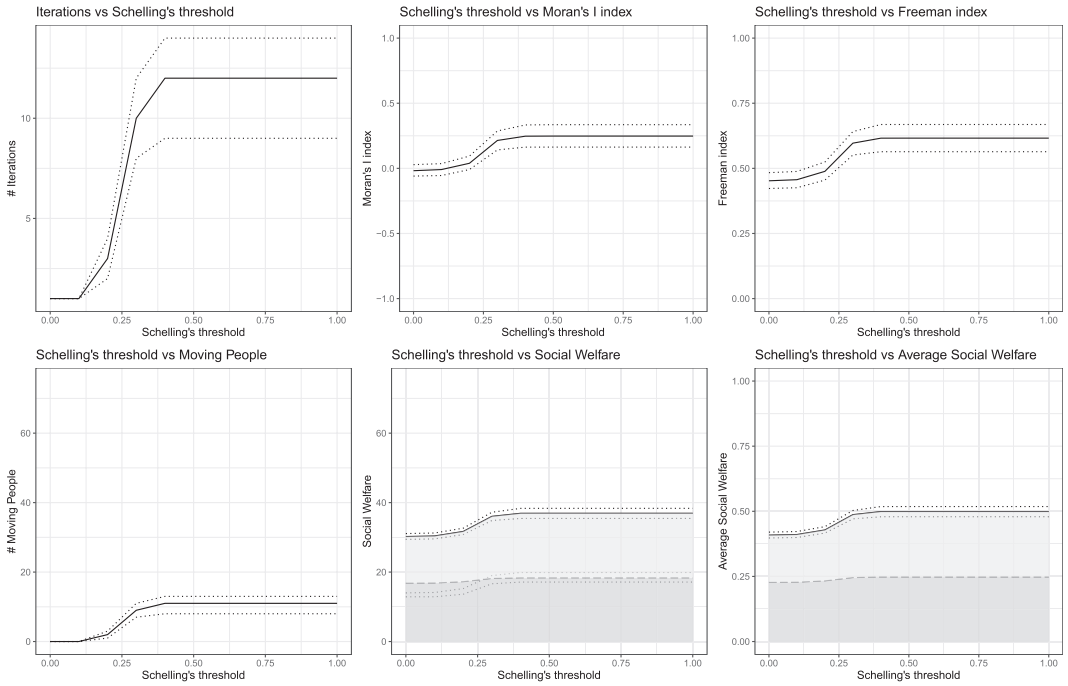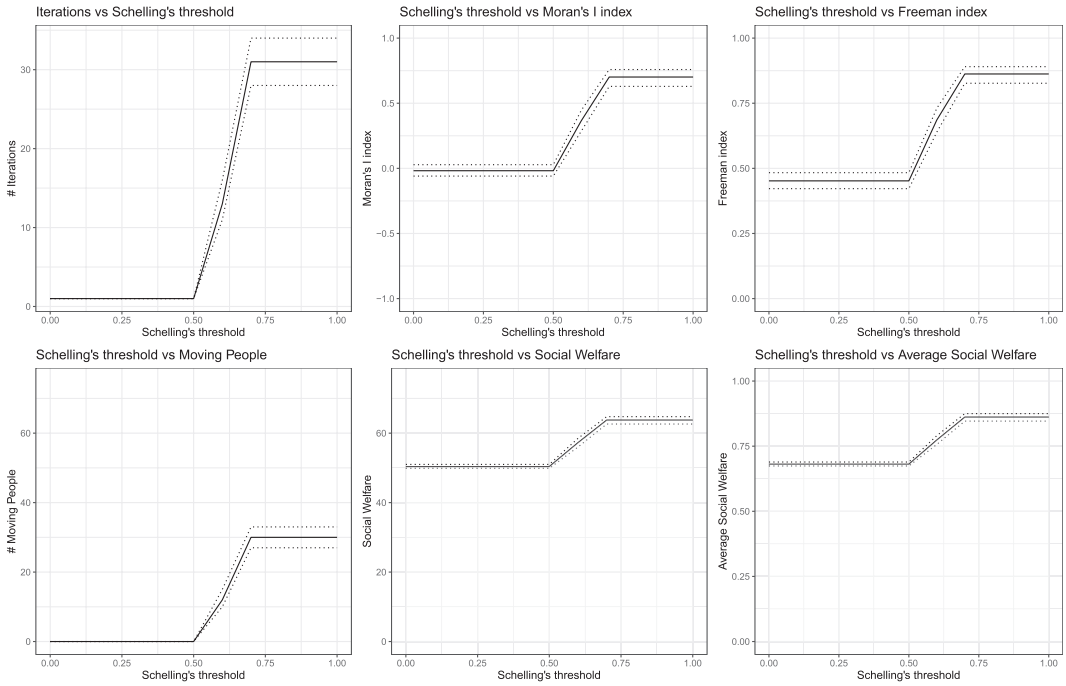
FIGURE B3 High fixed moving costs ($\beta = 0.5$, $\gamma = 1$, $\bar{c} = 0.99$)—No contribution of friendship to utility ($\alpha = 1$). Each simulation is repeated $H = 10{,}000$ times by permuting the initial torus. On the abscesses, we have Schelling's threshold x ranging in $[0, 1]$. Lines indicate, respectively, the second (lower ticked line), the third (bold line), and the fourth (upper ticked line) quintile of the distribution of values obtained. Upper left panel indicates the number of iterations required for the model to converge. Upper middle and right panels report, respectively, the Moran's I and the FSI value obtained after model convergence. Bottom left panel shows the number of people who moved at least once in a simulation. Bottom middle and right panels display, respectively, the average and the total social welfare of the agents at the end of the iteration process. Social welfare is obtained from the component $\beta\alpha U_i^{color}(\bar{v};x)$ of ith agent utility function (Equation 11)

FIGURE B4 High fixed moving costs ($\beta = 0.5, \gamma = 1, \bar{c} = 0.99$)—Fair contribution of friendship to utility and 3 friends ($\alpha = 0.5, k = 3$). Each simulation is repeated $H = 10{,}000$ times by permuting the initial torus. On the abscesses, we have Schelling's threshold x ranging in [0, 1]. Lines indicate, respectively, the second (lower ticked line), the third (bold line), and the fourth (upper ticked line) quintile of the distribution of values obtained. Upper left panel indicates the number of iterations required for the model to converge. Upper middle and right panels report, respectively, the Moran's I and the FSI value obtained after model convergence. Bottom left panel shows the number of people who moved at least once in a simulation. Bottom middle and right panels display, respectively, the average and the total social welfare of the agents at the end of the iteration process. Social welfare is obtained from the component $\beta\alpha U_i^{color}(\bar{v};x)$ of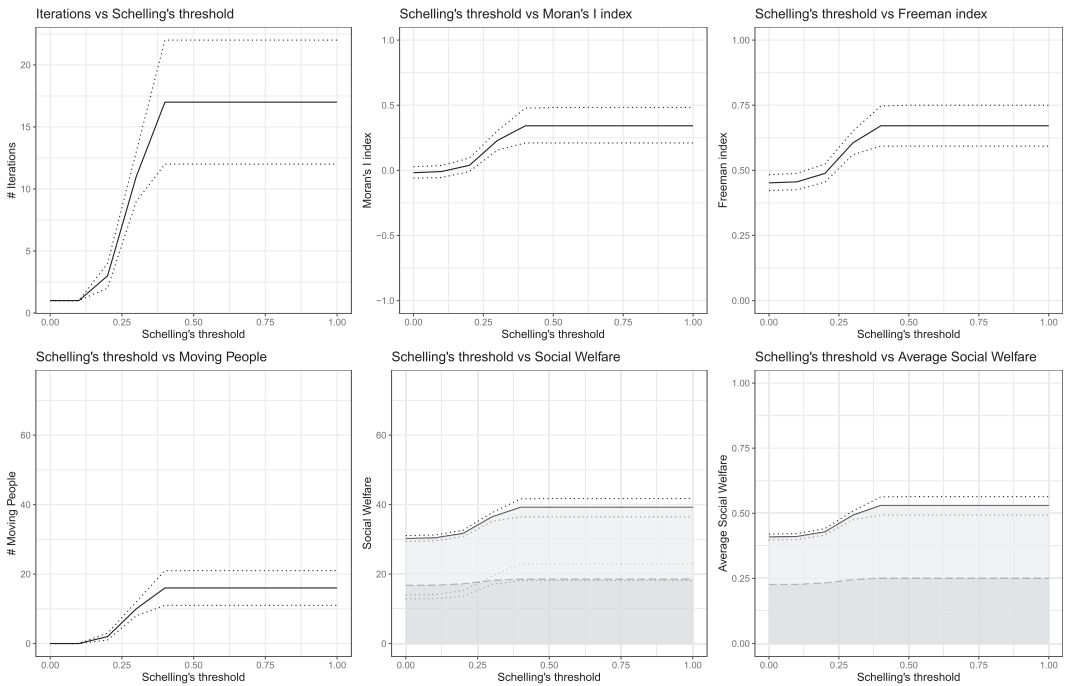 ith agent utility function (Equation 11). The color of the area indicates the two components of agents' utility after convergence is achieved: $\beta\alpha U_i^{color}(\bar{v};x)$ (lighter-colored area) and $\beta\alpha U_i^{friend}(\bar{v})$ (darker-colored area)
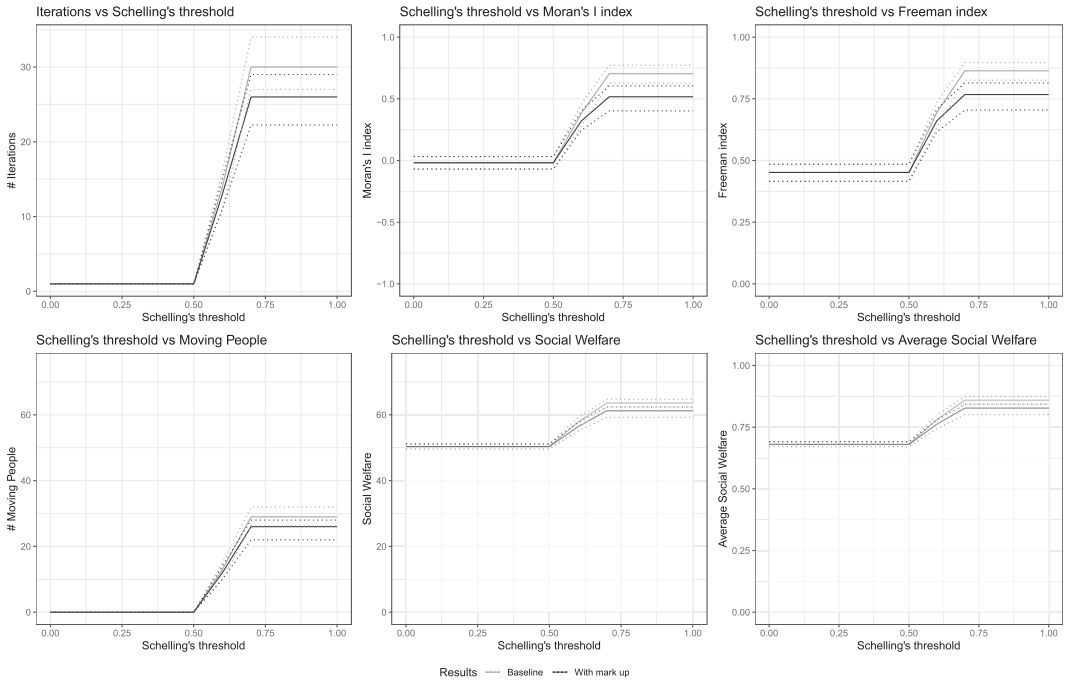
FIGURE B5 High variable moving costs ($\beta = 0.5$, $\gamma = 0$, $\overline{c} = 0.01$)—No contribution of friendship to utility ($\alpha = 1$). Each simulation is repeated $H = 10,000$ times by permuting the initial torus. On the abscesses, we have Schelling's threshold x ranging in [0, 1]. Lines indicate, respectively, the second (lower ticked line), the third (bold line), and the fourth (upper ticked line) quintile of the distribution of values obtained. Upper left panel indicates the number of iterations required for the model to converge. Upper middle and right panels report, respectively, the Moran's I and the FSI value obtained after model convergence. Bottom left panel shows the number of people who moved at least once in a simulation. Bottom middle and right panels display, respectively, the average and the total social welfare of the agents at the end of the iteration process. Social welfare is obtained from the component $\beta \alpha U_i^{color}(\overline{v};x)$ of ith agent utility function (Equation 11)

FIGURE B6 High variable moving costs ($\beta = 0.5,\ \gamma = 0,\ \bar{c} = 0.01$)—Fair contribution of friendship to utility and 3 friends ($\alpha = 0.5, k = 3$). Each simulation is repeated $H = 10{,}000$ times by permuting the initial torus. On the abscesses, we have Schelling's threshold x ranging in [0, 1]. Lines indicate, respectively, the second (lower ticked line), the third (bold line), and the fourth (upper ticked line) quintile of the distribution of values obtained. Upper left panel indicates the number of iterations required for the model to converge. Upper middle and right panels report, respectively, the Moran's I and the FSI value obtained after model convergence. Bottom left panel shows the number of people who moved at least once in a simulation. Bottom middle and right panels display, respectively, the average and the total social welfare of the agents at the end of the iteration process. Social welfare is obtained from the component $\beta\alpha U_i^{color}(\bar{v};x)$ of ith agent utility function (Equation 11). The color of the area indicates the two components of agents' utility after convergence is achieved: $\beta\alpha U_i^{color}(\bar{v};x)$ (lighter-colored area) and $\beta\alpha U_i^{friend}(\bar{v})$ (darker-colored area)

APPENDIX C

FIGURES: HETEROGENEOUS MOVING COSTS

FIGURE C1 Fixed moving costs ($\beta = 0.5$, $\gamma = 1$)—No contribution of friendship to utility ($\alpha = 1$). Each simulation is repeated $H = 10{,}000$ times by permuting the initial torus. On the abscesses, the Schelling's threshold x ranging in [0, 1]. Dark lines indicate, respectively, the second (lower ticked line), the third (bold line), and the fourth (upper ticked line) quintile of the distribution of values obtained of results obtained assuming the presence of two neighborhoods (each comprising 15% of the cells in the torus) where moving costs are subject to a mark up ($\bar{c} = 0.99$). Light lines indicate, respectively, the second (lower ticked line), the third (bold line), and the fourth (upper ticked line) quintile of the distribution of values obtained of baseline results, where moving costs are equal for all cells in the torus ($\bar{c} = 0.001$). Upper left panel indicates the number of iterations required for the model to converge. Upper middle and right panels report, respectively, the Moran's I and the FSI value obtained after model convergence. Bottom left panel shows the number of people who moved at least once in a simulation. Bottom middle and right panels display, respectively, the average and the total social welfare of the agents at the end of the iteration process. Social welfare is obtained from ith agent's utility function
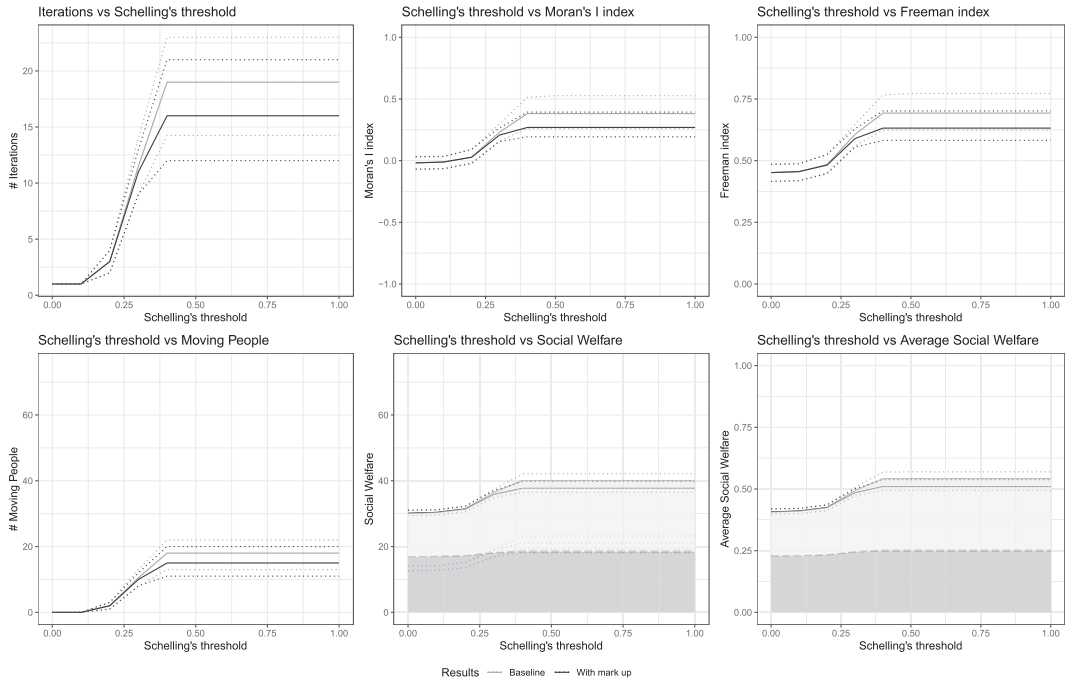
FIGURE C2 Fixed moving costs ($\beta = 0.5$, $\gamma = 1$)—fair utility from friendship and Schelling's heuristics ($\alpha = 0.5$)—3 friends ($k = 3$). Each simulation is repeated $H = 10,000$ times by permuting the initial torus. On the abscesses, the Schelling's threshold x ranging in [0, 1]. Dark lines indicate, respectively, the second (lower ticked line), the third (bold line), and the fourth (upper ticked line) quintile of the distribution of values obtained of results obtained assuming the presence of two neighborhoods (each comprising 15% of the cells in the torus) where moving costs are subject to a mark up ($\overline{c} = 0.99$). Light lines indicate, respectively, the second (lower ticked line), the third (bold line), and the fourth (upper ticked line) quintile of the distribution of values obtained of baseline results, where moving costs are equal for all cells in the torus ($\overline{c} = 0.001$). Upper left panel indicates the number of iterations required for the model to converge. Upper middle and right panels report, respectively, the Moran's I and the FSI value obtained after model convergence. Bottom left panel shows the number of people who moved at least once in a simulation. Bottom middle and right panels display, respectively, the average and the total social welfare of the agents at the end of the iteration process. Social welfare is obtained from ith agent's utility function. The color of the area indicates the two components of agents' utility after convergence is achieved: $\beta\alpha U_i^{color}(\overline{v};x)$ (lighter-colored area) and $\beta\alpha U_i^{friend}(\overline{v})$ (darker-colored area
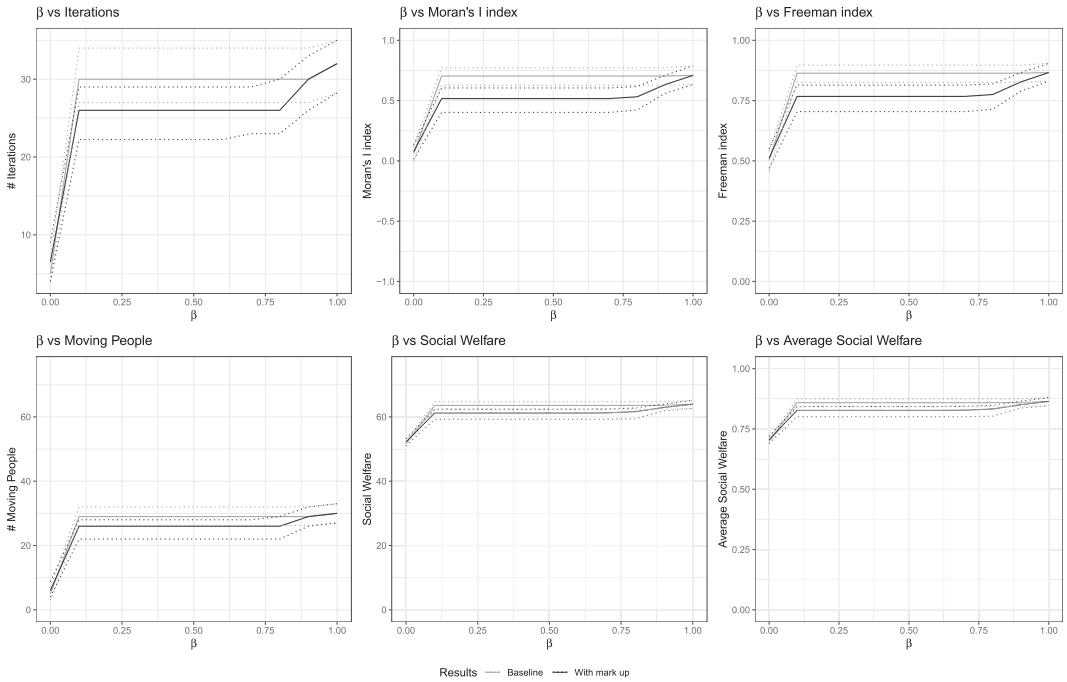
FIGURE C3 Fixed moving costs ($\gamma = 1$)—Maximum value of the Schelling's threshold $x = 1$—No contribution of friendship to utility ($\alpha = 1$). On the abscesses, the parameter β ranging in [0, 1]. Each simulation is repeated $H = 10{,}000$ times by permuting the initial torus. Dark lines indicate, respectively, the second (lower ticked line), the third (bold line), and the fourth (upper ticked line) quintile of the distribution of values obtained of results obtained assuming the presence of two neighborhoods (each comprising 15% of the cells in the torus) where moving costs are subject to a mark up ($\overline{c} = 0.99$). Light lines indicate, respectively, the second (lower ticked line), the third (bold line), and the fourth (upper ticked line) quintile of the distribution of values obtained of baseline results, where moving costs are equal for all cells in the torus ($\overline{c} = 0.001$). Upper left panel indicates the number of iterations required for the model to converge. Upper middle and right panels report, respectively, the Moran's I and the FSI value obtained after model convergence. Bottom left panel shows the number of people who moved at least once in a simulation. Bottom middle and right panels display, respectively, the average and the total social welfare of the agents at the end of the iteration process. Social welfare is obtained from the component $\beta\alpha U_i^{color}(\overline{v};x)$ of ith agent's utility function
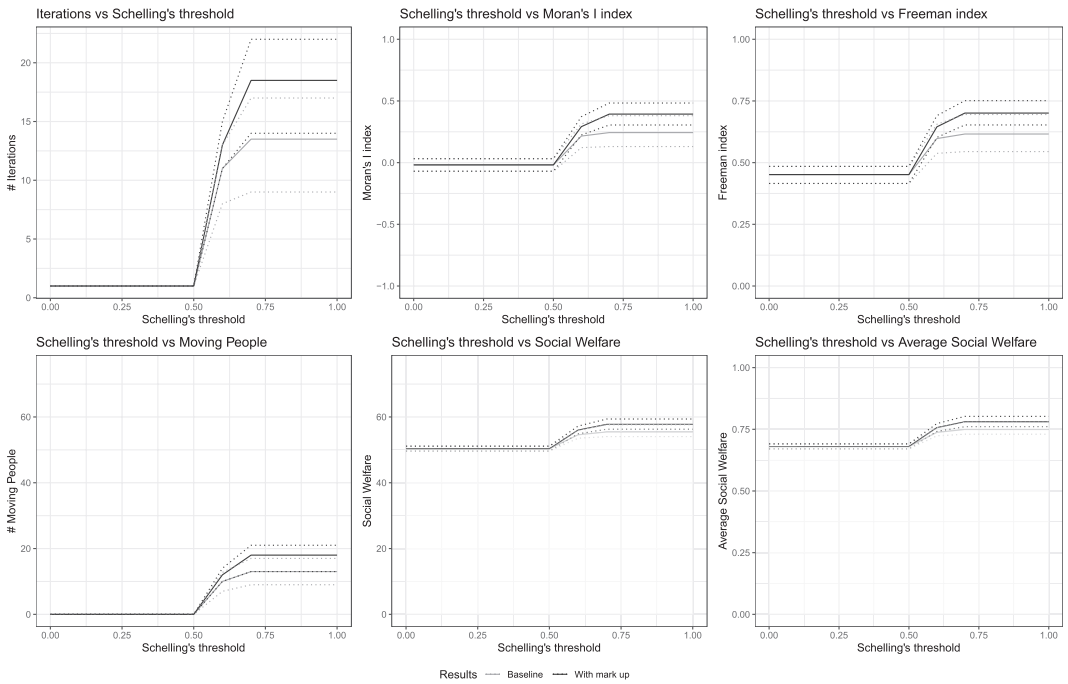
FIGURE C4 Variable moving costs ($\beta = 0.5$, $\gamma = 0$)—No contribution of friendship to utility ($\alpha = 1$). Each simulation is repeated $H = 10{,}000$ times by permuting the initial torus. On the abscesses, the Schelling's threshold x ranging in [0, 1]. Dark lines indicate, respectively, the second (lower ticked line), the third (bold line), and the fourth (upper ticked line) quintile of the distribution of values obtained of results obtained assuming the presence of two neighborhoods (each comprising 15% of the cells in the torus) where moving costs are subject to a mark up ($\overline{c} = 0.99$). Light lines indicate, respectively, the second (lower ticked line), the third (bold line), and the fourth (upper ticked line) quintile of the distribution of values obtained of baseline results, where moving costs are equal for all cells in the torus ($\overline{c} = 0.001$). Upper left panel indicates the number of iterations required for the model to converge. Upper middle and right panels report, respectively, the Moran's I and the FSI value obtained after model convergence. Bottom left panel shows the number of people who moved at least once in a simulation. Bottom middle and right panels display, respectively, the average and the total social welfare of the agents at the end of the iteration process. Social welfare is obtained from ith agent's utility function
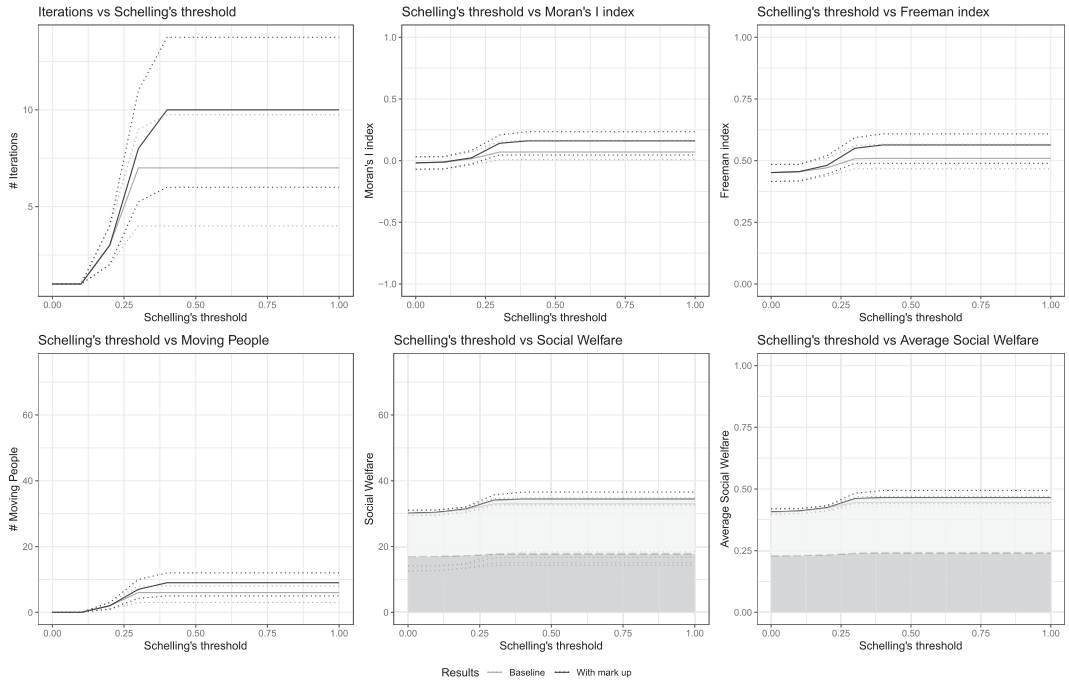
FIGURE C5 Variable moving costs ($\beta = 0.5$, $\gamma = 0$, $\overline{c} = 0.5$)—Fair utility from friendship and 3 friends ($\alpha = 0.5$, $k = 3$). Each simulation is repeated $H = 10,000$ times by permuting the initial torus. On the abscesses, the Schelling's threshold x ranging in $[0, 1]$. Dark lines indicate, respectively, the second (lower ticked line), the third (bold line), and the fourth (upper ticked line) quintile of the distribution of values obtained of results obtained assuming the presence of two neighborhoods (each comprising 15% of the cells in the torus) where moving costs are subject to a mark up ($\overline{c} = 0.99$). Light lines indicate, respectively, the second (lower ticked line), the third (bold line), and the fourth (upper ticked line) quintile of the distribution of values obtained of baseline results, where moving costs are equal for all cells in the torus ($\overline{c} = 0.001$). Upper middle and right panels report, respectively, the Moran's I and the FSI value obtained after model convergence. Bottom left panel shows the number of people who moved at least once in a simulation. Bottom middle and right panels display, respectively, the average and the total social welfare of the agents at the end of the iteration process. Social welfare is obtained from ith agent's utility function. The color of the area indicates the two components of agents' utility after convergence is achieved: $\beta \alpha U_i^{color}(\overline{v}; x)$ (lighter-colored area) and $\beta \alpha U_i^{friend}(\overline{v})$ (darker-colored area)
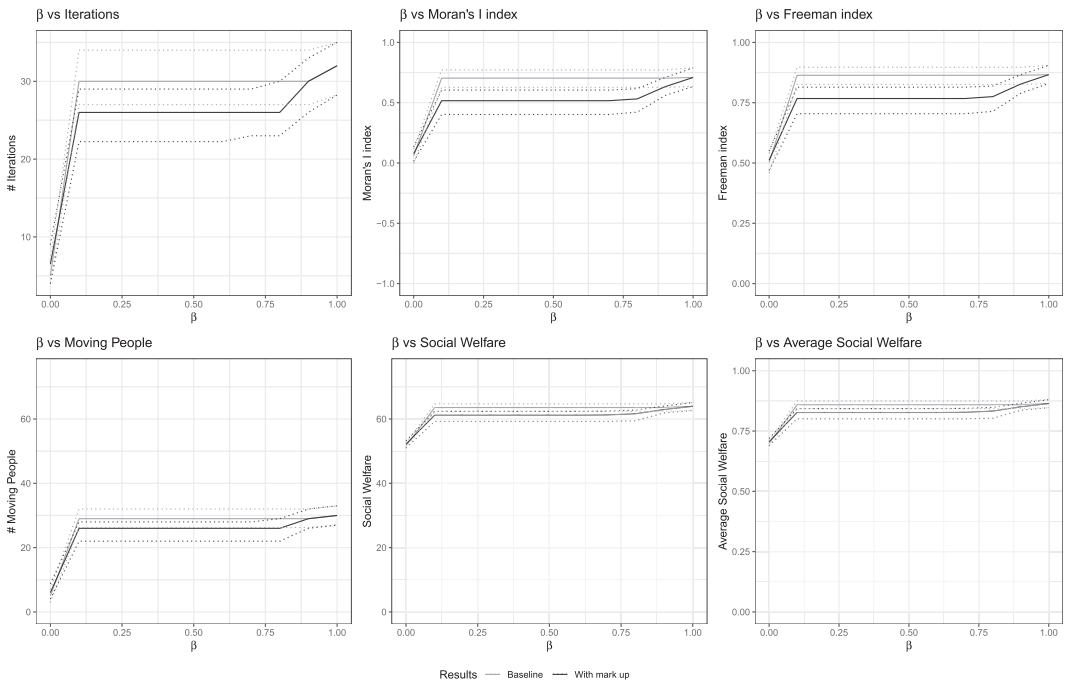
FIGURE C6 Variable moving costs ($\gamma = 0$)—Maximum value of the Schelling's threshold $x = 1$—No contribution of friendship to utility ($\alpha = 1$). On the abscesses, the parameter β ranging in $[0, 1]$. Each simulation is repeated $H = 10{,}000$ times by permuting the initial torus. Dark lines indicate, respectively, the second (lower ticked line), the third (bold line), and the fourth (upper ticked line) quintile of the distribution of values obtained of results obtained assuming the presence of two neighborhoods (each comprising 15% of the cells in the torus) where moving costs are subject to a mark up ($\overline{c} = 0.99$). Light lines indicate, respectively, the second (lower ticked line), the third (bold line), and the fourth (upper ticked line) quintile of the distribution of values obtained of baseline results, where moving costs are equal for all cells in the torus ($\overline{c} = 0.001$). Upper left panel indicates the number of iterations required for the model to converge. Upper middle and right panels report, respectively, the Moran's I and the FSI value obtained after model convergence. Bottom left panel shows the number of people who moved at least once in a simulation. Bottom middle and right panels display, respectively, the average and the total social welfare of the agents at the end of the iteration process. Social welfare is obtained from the component $\beta\alpha U_i^{color}(\overline{v};x)$ of ith agent's utility function

APPENDIX D

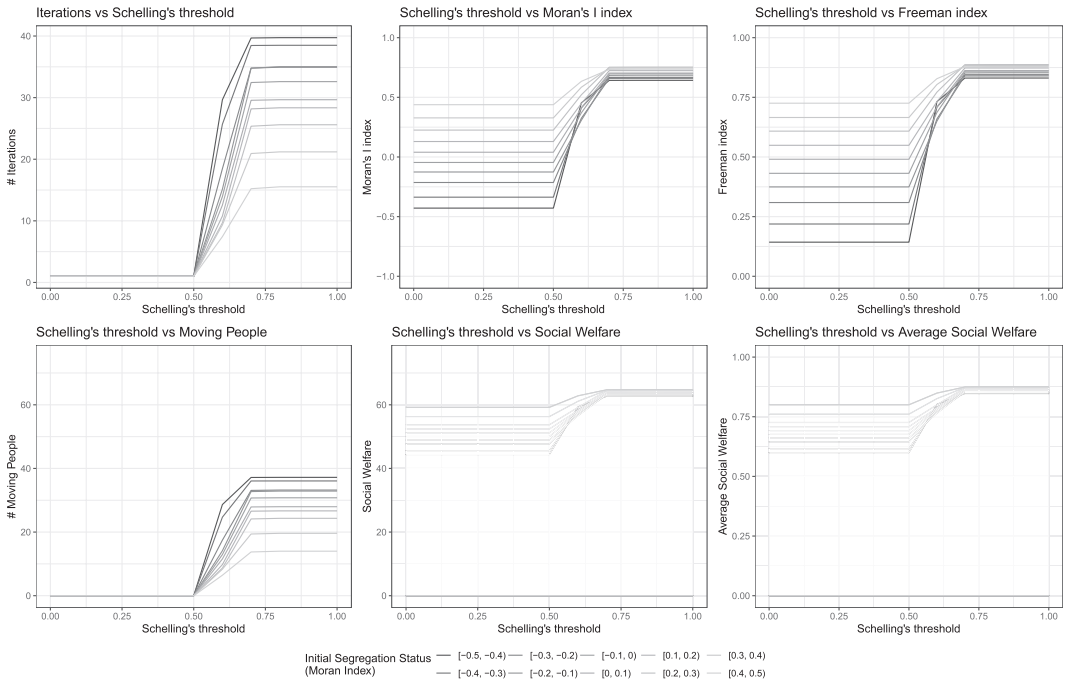## FIGURES: DIFFERENT INITIAL SEGREGATION STATUS

FIGURE D1 No moving costs ($\beta = 1$)—No contribution of friendship to utility ($\alpha = 1$). Each simulation is repeated $H = 10,000$ times by permuting the initial torus. On the abscesses, the Schelling's threshold x ranging in [0, 1]. Lines indicate the average value of each simulation results. Different colors indicate different initial segregation statuses of the torus. Upper left panel indicates the number of iterations required for the model to converge for different x values. Upper middle and right panels report, respectively, the Moran's I and the FSI value obtained after model convergence. Bottom left panel shows the number of people who moved at least once in a simulation. Bottom middle and right panels display, respectively, the average and the total social welfare of the agents at the end of the iteration process. Social welfare is obtained from the component $\beta\alpha U_i^{color}(\overline{v};x)$ of the ith agent utility function
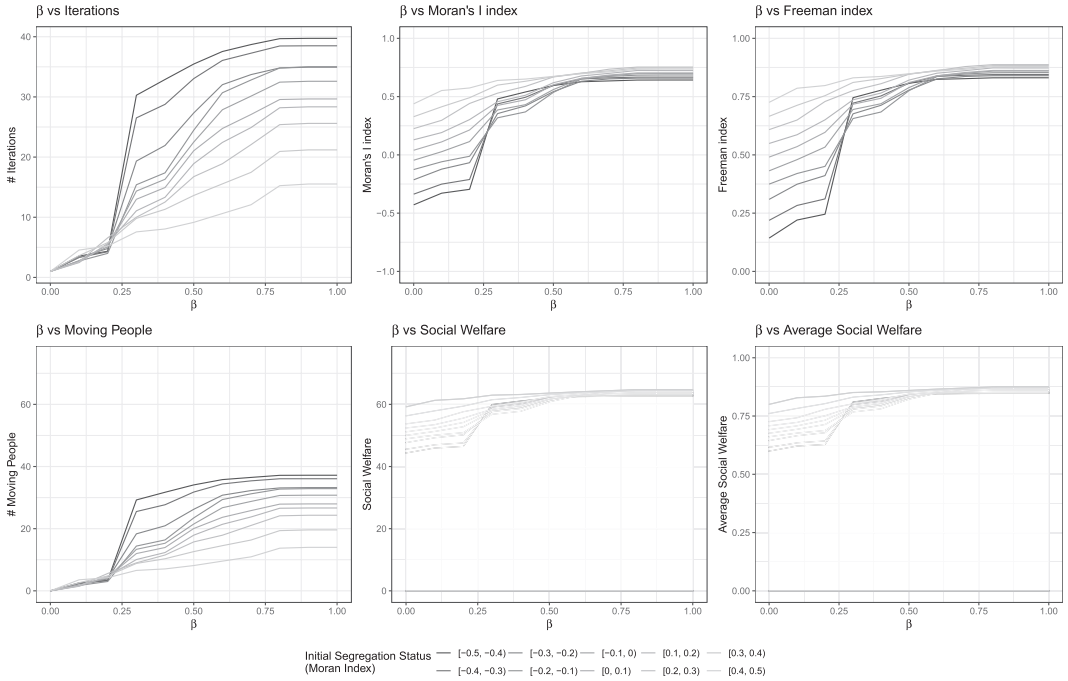
FIGURE D2 Fixed moving costs ($\gamma = 1$, $\bar{c} = 0.5$)—Maximum value of the Schelling's threshold $x = 1$—No contribution of friendship to utility ($\alpha = 1$). On the abscesses, the parameter β ranging in $[0, 1]$. Each simulation is repeated $H = 10,000$ times by permuting the initial torus. Lines indicate the average value of each simulation results. Different colors indicate different initial segregation statuses of the torus. Upper left panel indicates the number of iterations required for the model to converge. Upper middle and right panels report, respectively, the Moran's I and the FSI value obtained after model convergence. Bottom left panel shows the number of people who moved at least once in a simulation. Bottom middle and right panels display, respectively, the average and the total social welfare of the agents at the end of the iteration process. Social welfare is obtained from the component $\beta \alpha U_i^{color}(\bar{v};x)$ of ith agent's utility function
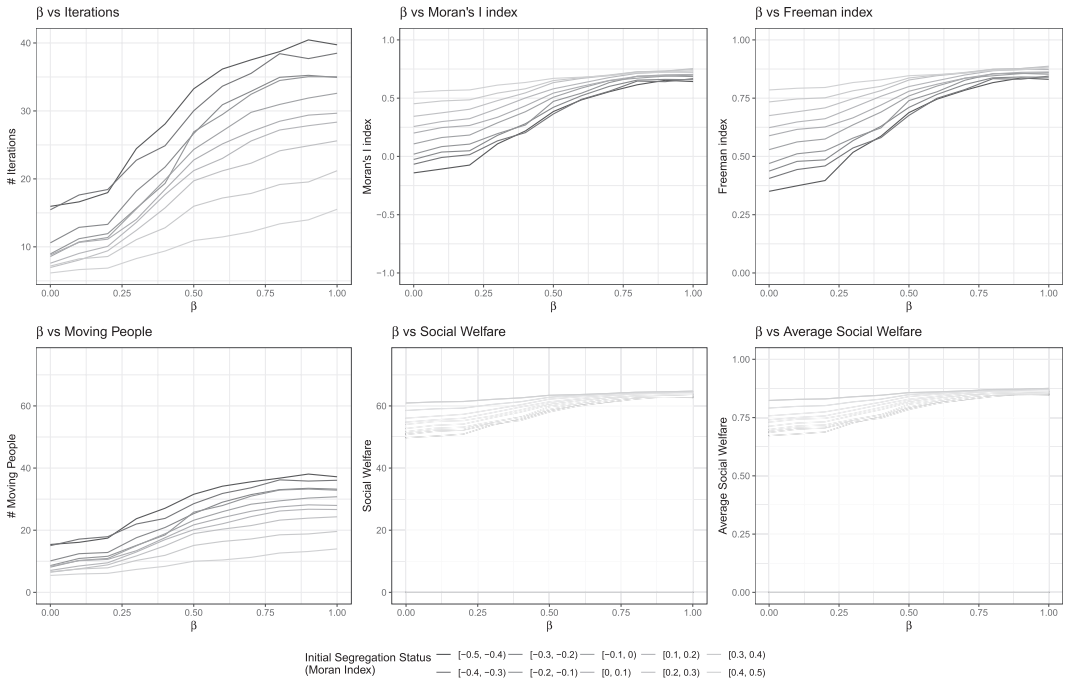
FIGURE D3 Variable moving costs ($\gamma = 0$, $\bar{c} = 0.5$)—Maximum value of the Schelling's threshold $x = 1$ —No contribution of friendship to utility ($\alpha = 1$). On the abscesses, the parameter β ranging in [0, 1]. Each simulation is repeated $H = 1000$ times by permuting the initial torus. Lines indicate the average value of each simulation results. Different colors indicate different initial segregation statuses of the torus. Upper left panel indicates the number of iterations required for the model to converge. Upper middle and right panels report, respectively, the Moran's I and the FSI value obtained after model convergence. Bottom left panel shows the number of people who moved at least once in a simulation. Bottom middle and right panels display, respectively, the average and the total social welfare of the agents at the end of the iteration process. Social welfare is obtained from the component $\beta\alpha U_i^{color}(\bar{v};x)$ of ith agent's utility function
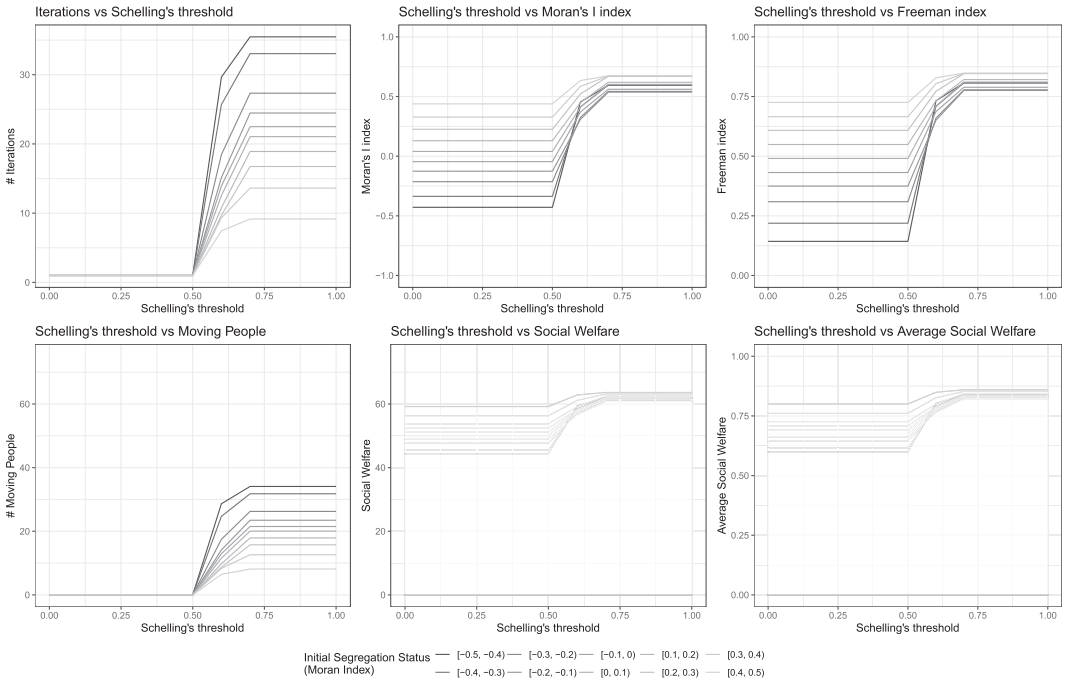
FIGURE D4 Fixed moving costs ($\beta = 0.5$, $\gamma = 1$, $\bar{c} = 0.5$)—No contribution of friendship to utility ($\alpha = 1$). Each simulation is repeated $H = 1000$ times by permuting the initial torus. On the abscesses, the Schelling's threshold x ranging in [0, 1]. Lines indicate the average value of each simulation results. Different colors indicate different initial segregation statuses of the torus. Upper left panel indicates the number of iterations required for the model to converge. Upper middle and right panels report, respectively, the Moran's I and the FSI value obtained after model convergence. Bottom left panel shows the number of people who moved at least once in a simulation. Bottom middle and right panels display, respectively, the average and the total social welfare of the agents at the end of the iteration process. Social welfare is obtained from ith agent's utility function
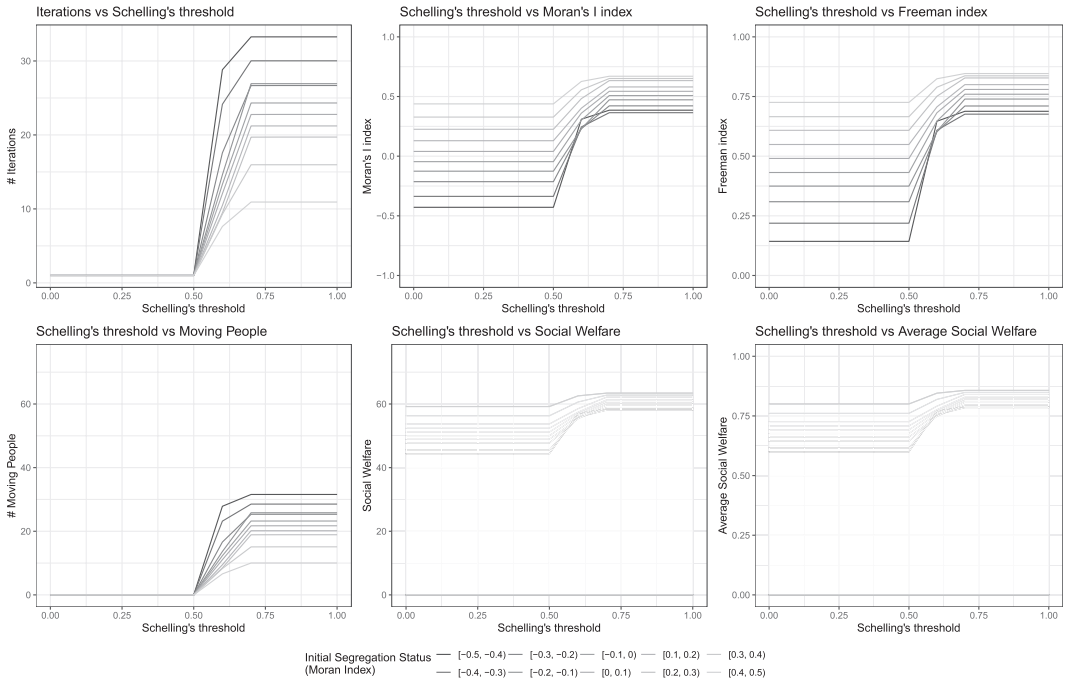
FIGURE D5 Variable moving costs ($\beta = 0.5$, $\gamma = 0$, $\bar{c} = 0.5$)—No contribution of friendship to utility ($\alpha = 1$). Each simulation is repeated $H = 1000$ times by permuting the initial torus. On the abscesses, the Schelling's threshold x ranging in [0, 1]. Lines indicate the average value of each simulation results. Different colors indicate different initial segregation statuses of the torus. Upper left panel indicates the number of iterations required for the model to converge. Upper middle and right panels report, respectively, the Moran's I and the FSI value obtained after model convergence. Bottom left panel shows the number of people who moved at least once in a simulation. Bottom middle and right panels display, respectively, the average and the total social welfare of the agents at the end of the iteration process. Social welfare is obtained from ith agent's utility function
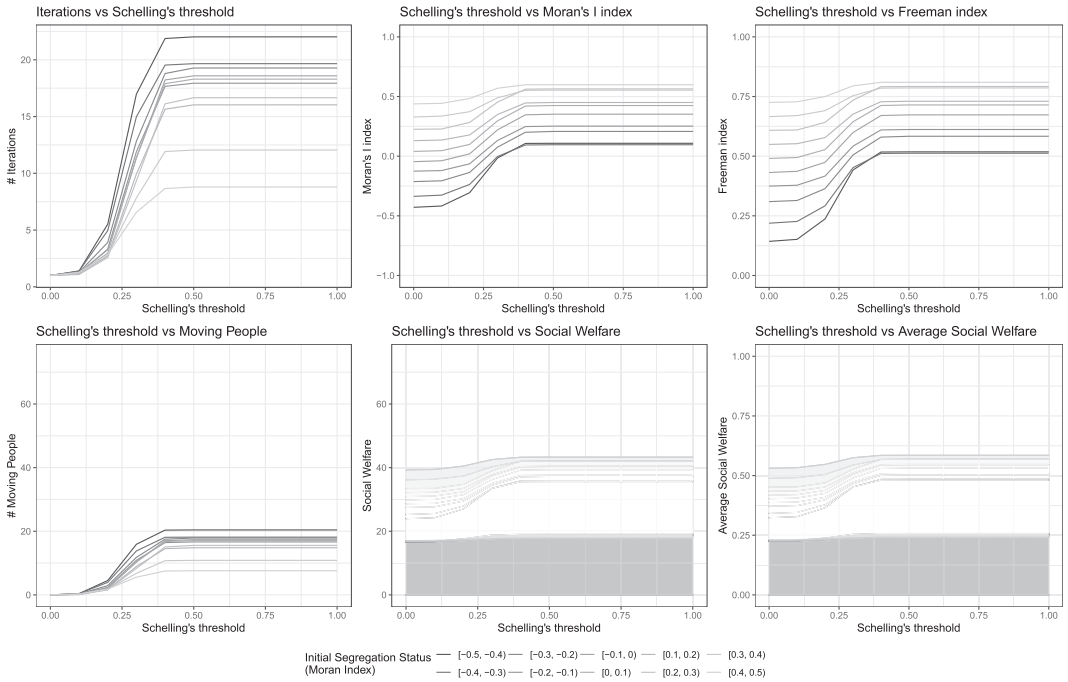
FIGURE D6   No moving costs ($\beta = 1$)—fair utility from friendship and Schelling's heuristics ($\alpha = 0.5$)—3 friends ($k = 3$) Each simulation is repeated $H = 1000$ times by permuting the initial torus and network connections. On the abscesses, the Schelling's threshold x ranging in [0, 1]. Lines indicate the average value of each simulation results. Different colors indicate different initial segregation statuses of the torus. Upper left panel indicates the number of iterations required for the model to converge. Upper middle and right panels report, respectively, the Moran's I and the FSI value obtained after model convergence. Bottom left panel shows the number of people who moved at least once in a simulation. Bottom middle and right panels display, respectively, the average and the total social welfare of the agents at the end of the iteration process. Social welfare is obtained from ith agent's utility function. The color of the area indicates the two components of agent's utility after convergence is achieved: $\beta\alpha U_i^{color}(\overline{v};x)$ (lighter-colored area) and $\beta\alpha U_i^{friend}(\overline{v})$ (darker-colored area
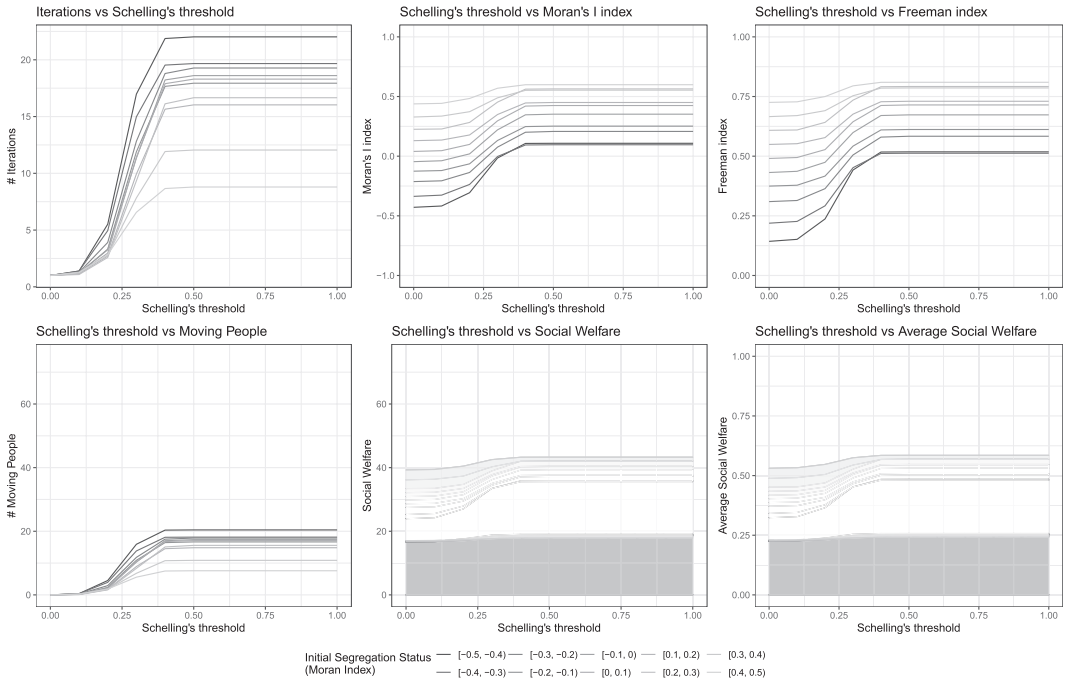
FIGURE D7 Fixed moving costs ($\beta = 0.5$, $\gamma = 1$, $\bar{c} = 0.5$)—fair utility from friendship and Schelling's heuristics ($\alpha = 0.5$)—3 friends ($k = 3$). Each simulation is repeated $H = 1000$ times by permuting the initial torus. On the abscesses, the Schelling's threshold x ranging in [0, 1]. Lines indicate the average value of each simulation results. Different colors indicate different initial segregation statuses of the torus. Upper left panel indicates the number of iterations required for the model to converge. Upper middle and right panels report, respectively, the Moran's I and the FSI value obtained after model convergence. Bottom left panel shows the number of people who moved at least once in a simulation. Bottom middle and right panels display, respectively, the average and the total social welfare of the agents at the end of the iteration process. Social welfare is obtained from ith agent's utility function. The color of the area indicates the two components of agents' utility after convergence is achieved: $\beta\alpha U_i^{color}(\bar{v};x)$ (lighter-colored area) and $\beta\alpha U_i^{friend}(\bar{v})$ (darker-colored area)
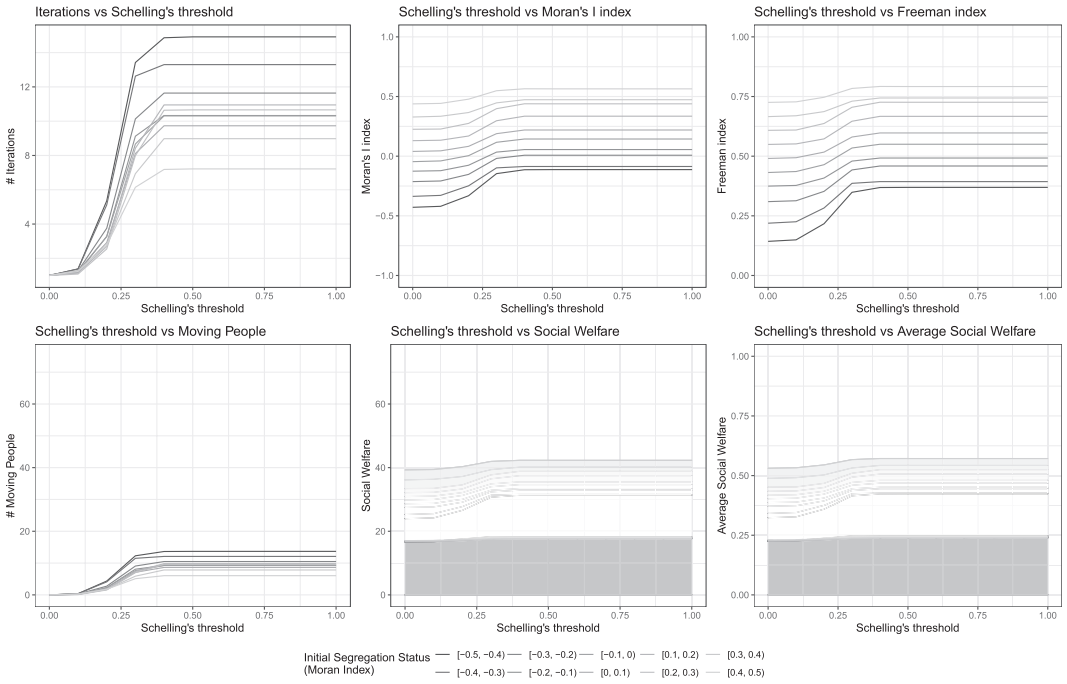
FIGURE D8 Variable moving costs ($\beta = 0.5$, $\gamma = 0$, $\bar{c} = 0.5$)—Fair utility from friendship and 3 friends ($\alpha = 0.5$, $k = 3$). Each simulation is repeated $H = 1000$ times by permuting the initial torus. On the abscisses, the Schelling's threshold x ranging in [0, 1]. Lines indicate the average value of each simulation results. Different colors indicate different initial segregation statuses of the torus. Upper left panel indicates the number of iterations required for the model to converge. Upper middle and right panels report, respectively, the Moran's I and the FSI value obtained after model convergence. Bottom left panel shows the number of people who moved at least once in a simulation. Bottom middle and right panels display, respectively, the average and the total social welfare of the agents at the end of the iteration process. Social welfare is obtained from ith agent's utility function. The color of the area indicates the two components of agents' utility after convergence is achieved: $\beta\alpha U_i^{color}(\bar{v};x)$ (lighter-colored area) and $\beta\alpha U_i^{friend}(\bar{v})$ (darker-colored area)
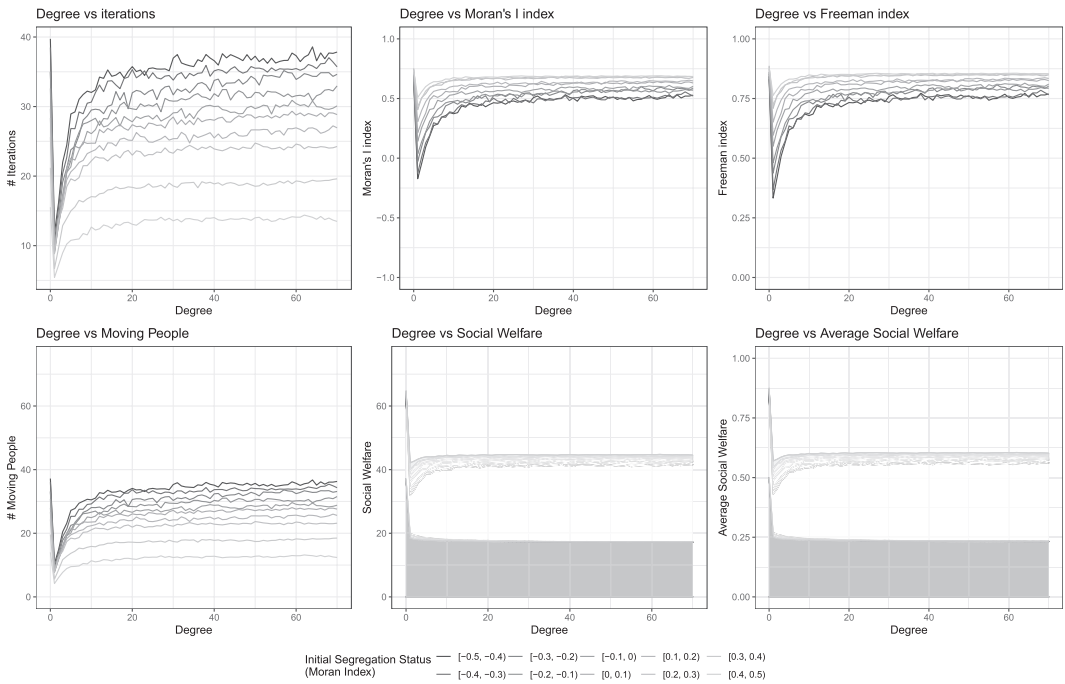
FIGURE D9 No moving costs ($\beta = 1$)—Fair contribution of friendship and Schelling's heuristics to utility ($\alpha = 0.5$)—Maximum value of the Schelling's threshold $x = 1$. Each simulation is repeated $H = 1000$ times by permuting the initial torus and network connections. On the abscisses, the degree centrality (number of friends) k, ranging from 0 to 73. Lines indicate the average value of each simulation results. Different colors indicate different initial segregation statuses of the torus. Upper left panel indicates the number of iterations required for the model to converge. Upper middle and right panels report, respectively, the Moran's I and the FSI value obtained after model convergence. Bottom left panel shows the number of people who moved at least once in a simulation. Bottom middle and right panels display, respectively, the average and the total social welfare of the agents at the end of the iteration process. Social welfare is obtained from agents' utility function. The color of the area indicates the two components of agents' utility after convergence is achieved: $\beta\alpha U_i^{color}(\overline{v};x)$ (lighter-colored area) and $\beta\alpha U_i^{friend}(\overline{v})$ (darker-colored area)